

# **Adsorption of Cd(II) and Pb(II) ions from aqueous solutions using mesoporous activated carbon adsorbent: Equilibrium, kinetics and characterisation studies.**

Edidiong Asuquo <sup>1\*</sup>; Alastair Martin<sup>1, 2</sup>; Petrus Nzerem<sup>1, 3</sup>; Flor Siperstein<sup>1</sup> and Xiaolei Fan<sup>1</sup>

<sup>1</sup>School of Chemical Engineering and Analytical Science, The Mill, Sackville Street, University of Manchester, Manchester, M13 9PL, United Kingdom.

<sup>2</sup>Alastair Martin -Present address-

Department of Engineering, Lancaster University, Bailrigg, Lancaster  
LA1 4YR. United Kingdom

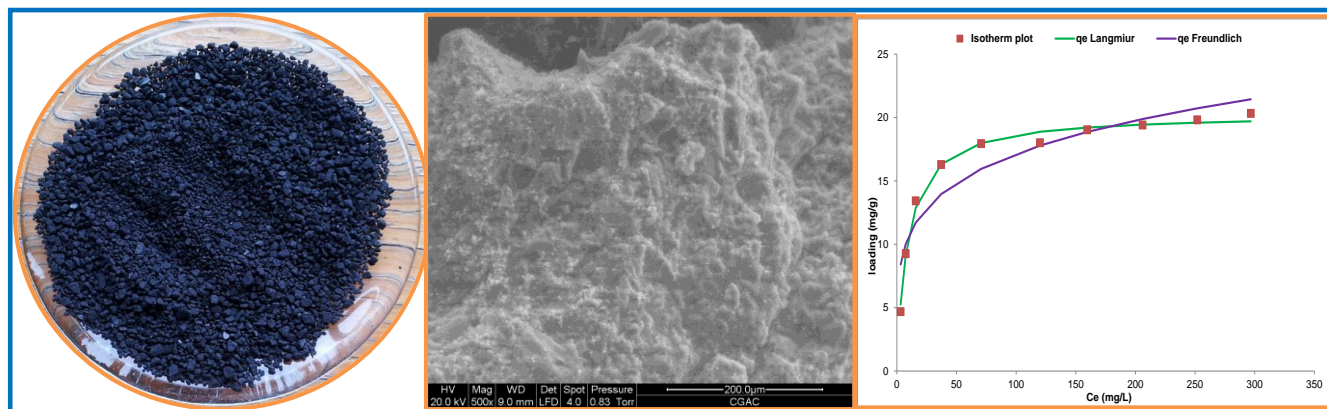
<sup>3</sup>Petrus Nzerem -Present address-

Department of Chemistry, Nigerian Turkish Nile University, Research Institution Area  
Abuja, Nigeria.

\*Corresponding author. +441612003975

E-mail address: [edidiong.asuquo@postgrad.manchester.ac.uk](mailto:edidiong.asuquo@postgrad.manchester.ac.uk)

## Graphical Abstract



## Highlights

- High surface area commercial adsorbent used for Cd(II) and Pb(II) sorption
- Kinetic profile indicated a rapid uptake within 30 minutes for both metals
- Kinetic modelling indicated pseudo-first order described Pb(II) and pseudo-second order described Cd(II) sorption
- Langmuir model gave better description of Cd(II) and Pb(II) ions sorption

## Abstract

In this study, cadmium and lead ions removal from aqueous solutions using a commercial activated carbon adsorbent (CGAC) were investigated under batch conditions. The adsorbent was observed to have a coarse surface with crevices, high resistance to attrition, high surface area and pore volume with bimodal pore size distribution which indicates that the material was mesoporous. Sorption kinetics for Cd(II) and Pb(II) ions proceeded through a two-stage kinetic profile- initial quick uptake occurring within 30 minutes followed by a gradual removal of the two metal ions until 180 minutes with optimum uptake ( $q_{e,exp}$ ) of  $17.23 \text{ mgg}^{-1}$  and  $16.84 \text{ mgg}^{-1}$  for Cd(II) and Pb(II) ions respectively. Modelling of sorption kinetics indicates that the pseudo first order (PFO) model described the sorption of Pb(II) ion better than Cd(II), while the reverse was observed with respect to the pseudo second order (PSO) model. Intraparticle diffusion modelling showed that intraparticle diffusion may not be the only mechanism that influenced the rate of ions uptake. Isotherm modelling was carried out and the results indicated that the Langmuir and Freundlich models described the uptake of Pb(II) ion better than Cd(II) ion. A comparison of the two models indicated that the Langmuir isotherm is the better isotherm for the description of Cd(II) and Pb(II) ions sorption by the adsorbent. The maximum loading capacity ( $q_{max}$ ) obtained from the Langmuir isotherm was  $27.3 \text{ mgg}^{-1}$  and  $20.3 \text{ mgg}^{-1}$  for Cd(II) and Pb(II) ions respectively.

**Keywords:** Adsorption, commercial activated carbon, adsorbent, lead, cadmium, heavy metals, kinetics, isotherm

## 1. Introduction

The advent of industrialization and the increasing rate of consumption in our society has brought with it increased levels of industrial pollution resulting in a significant level of ecosystem destruction with high pollutant concentrations such as heavy metals and organic compounds in water resources raising global concern on the threat posed by industrial activities on the environment (Park *et al.*, 2006). A large proportion of water pollutants that affect our environment results from industrial activities and their ever increasing nature have led to the present state of our global environment. This is because of the huge chemical input associated with these processes and the inefficient resource utilization of the input components leads to huge generation of waste streams that require disposal into the environment. The low efficiency of the treatment processes used in these industrial sites for the treatment of industrial effluents further increases the pollutant load in treated discharged effluents. Thus, wastewater from these industrial activities is mostly contaminated with organic and inorganic pollutants amongst which are heavy metal ions, phosphates, sulphates, organic and hydrocarbon compounds. Some of these compounds are known as priority pollutants in many waste streams such as those originating from industrial activities relating to petroleum production, refining and petrochemicals, pulp and paper manufacture, battery manufacture, tanneries, paint and pigment industries, fertilizer, herbicide and pesticide industries as well as mining and metallurgical plants (Pamukoglu and Kargi, 2007; Ho and Ofomaja, 2006; Bailey *et al.*, 1999).

Amongst the list of pollutants that affect our environment, heavy metals are becoming more prominent due to the diverse routes of its exposure, its toxic implications across time scales and the level of industrial development in recent decades. The main source of input of heavy metals into the environment has been from industrial activities which lead to challenges in their reduction and remediation. Since these heavy metals possess diverse toxicity and are not biodegradable, their toxic impact may develop over a long period of time as is the case in closed mines or mining sites that have fallen into disrepair and abandoned. This may lead to a variety of chemical speciation of these heavy metals in the soil, air and water environments and with different routes of exposure their toxic implications are magnified over a long time due to their long half-lives (Nurchi and Villaescusa, 2008).

Lead and cadmium are two common toxic heavy metals that man is increasingly being exposed to due to their properties and wide applications in materials and technologies that define human survival. For example lead metal is used in the construction and building industry as a

component of metal alloys and in the nuclear industry as a radiation shield. Lead is also relevant in the electroplating industry, textile industry, metal processing and finishing, as solders with tin (Sn), fusible alloys, storage batteries (lead-acid car battery), explosive materials, photographic materials and fuel additives (Tong *et al.*, 2000; ASTDR, 2007; Gerçel and Gerçel, 2007). Lead pigments are used in a variety of applications like chromate for road markings and oxides for glass and chemicals. Cadmium is used for the manufacture of the following materials; batteries; pigments; coatings and platings; stabilizers for plastics; nonferrous alloys and photovoltaic devices (ASTDR, 2012). Cadmium is released into the environment in a variety of ways such as tobacco smoking, mining, smelting and refining of non-ferrous metals; fossil fuel combustion, incineration of municipal waste (especially cadmium-containing batteries and plastics), metal plating industries, manufacture of phosphate fertilizers, recycling of cadmium-plated steel scrap as well as electric and electronic waste (WHO, 2010, Xi *et al.*, 2015; USEPA, 2016).

Due to their widespread use, these two metals can have toxic effects on humans as well as flora and fauna. Human exposure to lead ions can be from lead dust which originates from the degradation of lead paints and other routes including drinking contaminated water from lead pipes. Due to accumulation of lead in the environment from anthropogenic sources, human exposure to lead ions has become a problem in the society in both developing and developed countries. Lead speciation also affects the rate of absorption as the human body is known to absorb organic lead faster than inorganic lead. Lead is a heavy metal poison that affects the functioning of the blood, liver, kidney and brain of the human being (Tong *et al.*, 2000). It is known as a large cation especially prone to react with sulfhydryl (-SH) groups in proteins in a manner similar to cadmium ions. It acts by complexing with oxo-groups in enzymes affecting virtually all steps in the process of heme-synthesis and porphyrin metabolism (ATSDR, 2010; Greenwood and Earnshaw, 2006). At high concentrations lead is known to cause encephalopathy, cognitive impairment, kidney and liver damage, anaemia and toxicity to the reproductive system (Pagliuca and Mufti, 1990; O'Connell *et al.*, 2008; Adekunle *et al.*, 2014). The USEPA discharge limit for lead in effluents is  $0.005 \text{ mgL}^{-1}$ , while the limit for discharged effluents into aquatic water by the World Health Organisation (WHO) is  $0.01 \text{ mgL}^{-1}$  (Bhattacharjee *et al.*, 2003; Ipeaiyeda and Onianwan, 2011; Gerçel and Gerçel, 2007).

Cadmium is an element with no known positive biological function on humans and is one of the most serious environmental pollutants especially in the vicinity of smelters. It has a high affinity for sulfhydryl (-SH) groups of proteins for which it competes with Zn(II) in biological systems

and is known as a human carcinogen (WHO, 2010). Due to its low-concentration-long-term effect in drinking water, cadmium belongs to the chemicals list of endocrine disruptors and priority control pollutants issued by USEPA (Waisberg *et al.*, 2003; Huang *et al.*, 2007). The toxic implications of cadmium in the environment has made the US Environmental protection Agency (USEPA) to set the level of cadmium in drinking water to  $0.002 \text{ mgL}^{-1}$  and the World Health Organisation (WHO) maximum permissible limit for cadmium in drinking water is  $0.003 \text{ mgL}^{-1}$  (USEPA, 2016; WHO, 2010; Rao *et al.*, 2010; Xi *et al.*, 2015; WHO, 2011).

Due to the toxic implications of these two metals, approaches that promote their removal from aqueous effluents have been classified as priority in the last two decades and a number of technologies have been explored (Dzul Erosa, *et al.*, 2001). The use of adsorption has become one of the techniques explored in recent years. A number of materials have been synthesised and used for the adsorption of Cd(II) and Pb(II) ions such as amino propyl-modified mesoporous carbon (Hamad *et al.*, 2016); chemically modified polyacrylonitrile-based fiber (Deng *et al.*, 2016) and spherical mesoporous silica (Zhu *et al.*, 2016; Li *et al.*, 2016). In spite of these advances in material synthesis for adsorption of pollutants such as heavy metals, the material at the forefront of adsorption technology is still activated carbon. Activated carbon has gained widespread use for the treatment of heavy metal ions and other pollutants because of its inherent physical properties such as large surface area, porous structure, high adsorption capacity and large reactive surface (Khah and Ansari, 2009; Shrestha *et al.*, 2013; Arena *et al.*, 2016). It is widely used due to its exceptional high surface area (ranges from  $500$  to  $5000 \text{ m}^2\text{g}^{-1}$ ), well developed microporosity and wide spectrum of surface functional groups. These properties of activated carbon are generally controlled by the manufacturing process which depends on the nature of raw materials, activating agents and conditions of activation (Rivera- Utila *et al.*, 2011; Selomulya *et al.*, 1999; Khah and Ansari, 2009).

Commercial activated carbon is often the preferred adsorbent for the removal of pollutants due to its versatile nature for a wide variety of compounds; however its widespread use is often restricted due to high associated cost. This has driven research into the use of inexpensive alternative activated carbon precursors such as waste materials from agriculture, wood and fisheries industry (Dias *et al.*, 2007). This drive in research on low cost precursors for the synthesis of activated carbon has led to an exponential increase in studies reporting the use of these activated carbon adsorbents obtained from waste materials for the removal of both organic and inorganic pollutants. This research platform also requires that studies on the use of the commercial activated carbon for the removal of the target pollutants that are of interest in the

environment should also be undertaken to serve as a standard for comparing the low cost based activated carbon adsorbents obtained from waste precursors. This will provide information that is significant for the commercial exploitation of the synthesis of activated carbon adsorbents from low cost precursors. In this regard, more studies have been reported in literature with focus on the removal of organic pollutants such as dyes, phenols, volatile organic compounds than heavy metal ions using commercial activated carbon (Dias *et al.*, 2007; Ahmedna *et al.*, 2000; El-Shafey *et al.*, 2016; Al-Lagtah *et al.*, 2016). The increasing environmental and health challenges posed by toxic heavy metal pollution as the advancement in industrialisation reaches the shores of the developing economies requires that more investigations should be carried out with respect to the use of commercial activated carbon adsorbents for those heavy metal ions that are prevalent in these countries.

Hence, this study is designed to provide information on the use of a commercial activated carbon adsorbent for the removal of two prominent heavy metals that are toxic and are prevalent in developing economies as a result of their drive towards industrialisation. A commercially manufactured activated carbon (Chemviron Carbon) was used as adsorbent for this study. Characterisation of both physical and chemical properties of the commercial activated carbon (CGAC) will be investigated to give insight on the material and this will be used to correlate with the ions uptake in aqueous phase. In addition, Cd(II) and Pb(II) ions kinetic and equilibrium sorption as well as the modelling of the transport of the two ions onto the surface of the commercial activated carbon will be investigated.

## **2. Materials and methods**

### **2.1 Chemicals and adsorbent**

Standard stock solutions of  $1000 \text{ mgL}^{-1}$  of the two metal ions were prepared by dissolving appropriate amounts of analytical grade reagent [cadmium nitrate tetrahydrate-Cd  $(\text{NO}_3)_2 \cdot 4\text{H}_2\text{O}$  (Sigma-Aldrich) (99% assay)] and [Pb(II) nitrate-Pb $(\text{NO}_3)_2$  (Sigma-Aldrich) (99% assay)] in deionised water using a 1000 mL volumetric flask (MBL Boro England). The stock solutions were acidified to prevent hydrolysis by adding 5mL  $\text{HNO}_3$  and the volume was made up to the 1000 mL. The content of each volumetric flask was agitated in a Heidolph Unimax instrument 1010 shaker at 300 rpm for 3 h to ensure complete dissolution at room temperature ( $25^\circ\text{C}$ ). A commercial activated carbon (granular, diameter  $> 425\mu\text{m}$ ) purchased from Chemviron Carbon (sample F-400), which is an agglomerated coal based granular activated carbon was the

adsorbent used in this study. It was used as received without any further pre-treatment and labelled as commercial activated carbon adsorbent (CGAC) for the sorption of Cd(II) and Pb(II) ions.

## 2.2 Instruments and adsorbent characterisation

The surface morphology of the CGAC adsorbent before and after Cd(II) and Pb(II) ion adsorption as well as their chemical composition were analysed by scanning electron microscopy (SEM) and energy dispersive X-ray analysis (EDX). The equipment used for the SEM and EDX analysis was a FEI Quanta 200 Environmental Scanning Electron Microscope. The CGAC adsorbents were placed and pressed onto carbon tabs (9mm-Agar Scientific) and mounted on a 0.5" SEM pin stubs (Agar Scientific) of length 6mm. The samples were preconditioned for analysis by coating using an EMITECH K550X sputter gold coater and coating was carried out for 15 minutes and thereafter analysed in the vacuum chamber. The surface area and porosity of the CGAC adsorbent was determined using a Micromeritics Tristar 3000 Surface Area and Porosity Analyzer. The CGAC adsorbent was pre-conditioned by drying in an oven for 24 h at 150°C after which it was weighed into the BET sample tube and conditioned (degassed) for 2 hr at 200°C under nitrogen flow in order to eliminate moisture and other gases on the adsorbent using the *Micromeritics Flow prep 060 sample degas system*. Thereafter it was cooled under nitrogen flow for 5 minutes in the cooling section of the Flow prep system and when it had cooled it was then weighed again to determine the actual weight of sample to be analysed prior to the analysis using the Micromeritics Tristar 3000 Surface Area and Porosity Analyzer. The bulk density of the CGAC was determined using the procedure reported by Lima and Marshall (2005). The adsorbent was dried for 24h at 100 °C before analysis. A graduated 25mL glass cylinder was filled to a given volume with a known weight of the adsorbent; the cylinder was capped and tapped to a constant minimum volume to compact the adsorbent for 2 minutes. The bulk density ( $\text{g cm}^{-3}$ ) was calculated as the ratio between the weight of the adsorbent and the volume of the cylinder occupied. The gravimetric change with temperature of the CGAC adsorbent was determined by a thermogravimetric analyzer (TGA Q5000-TA instrument). A known mass of the sample was weighed onto a ceramic pan and subjected to temperature profile analysis from 30°C to 590°C under nitrogen atmosphere to monitor the thermal degradation at a heating rate of  $10^\circ\text{C min}^{-1}$  for 60 minutes. The nitrogen flow rate was kept at  $50 \text{ mL min}^{-1}$ .

The acidic/basic character of each adsorbent in an aqueous system was estimated by pH measurement of the suspensions according to the following methods using deionized water, 18.2 M $\Omega$  cm<sup>-1</sup> (Millipore). Preparation of CO<sub>2</sub>-free deionized water was carried out by boiling 200 mL of deionized water for 60 minutes and allowing the water to cool. Thereafter, the 0.5 g of the CGAC adsorbent was weighed into 25 mL of the degassed water in a sealed conical flask and constantly agitated for 24 h at room temperature (25°C). Subsequently, the pH of the CGAC adsorbent mixture after 24 h was determined using an accumet<sup>(R)</sup> pH-meter (Fisher-Scientific). The measurement was carried out in triplicates and the average value taken as the pH of the CGAC adsorbent mixture. The point of zero charge (pHpzc) of the CGAC adsorbent was determined using the Malvern Zetasizer. The equipment used was a Zetasizer 3000 HSA by Malvern Instruments. The samples were prepared by weighing 0.1 g of sample into 20 mL of 0.01 M NaCl solution at pH range of 2 – 12 and agitating it in a shaker for 24 h. After which it was filtered and 10 mL of each filtrate was taken out and put in a polypropylene bottle for analysis. The Zetasizer syringe was first of all cleaned and the analysis cell purged with deionized water using the syringe. The samples of each of the adsorbents at different pH were inserted into the Zetasizer electrophoresis cell using a syringe and the sample inserted into a 3 mL polystyrene curvette with a light path of 10 mm. The zeta potential at each pH was measured and recorded. Three measurements were carried out and an average zeta potential for each adsorbent suspension at the different pH values were recorded. Fourier transform infra-red spectroscopy was used to evaluate the functional groups in the CGAC adsorbent before and after Cd(II) and Pb(II) ion sorption. The infra-red spectra were collected using an attenuated total reflectance FT-IR spectroscopy (ATR-FT-IR) in absorbance mode. The instrument used was the Bruker- ALPHA FT-IR with platinum ATR probe. The spectra range was from 4000 – 400 cm<sup>-1</sup> and the spectra were collected using the FTIR-ATR spectrometer using a total average of 32 co-added scans and a spectral resolution of 4 cm<sup>-1</sup> with background subtraction.

The attrition resistance of the CGAC adsorbent was determined using a modification of the wet attrition test procedure (Lima and Marshall, 2005). Two grams (2 g) of each adsorbent was weighed into a 20 mesh screen and 1 g of the amount retained on the mesh was weighed into a 250 mL Erlenmeyer flask. 100 mL deionized water was thereafter added to the flask and the suspension stirred for 24 h at 25°C on a magnetic stirrer at 200 rpm using ½ inch magnetic stir bars. After 24 h the suspension was poured into a 20 mesh screen and the retained adsorbent dried in an oven of 100°C for 24 h. Thereafter, the dried CGAC adsorbent was weighed using a Mettler Sauter RL 200 electric weighing balance (August Sauter GmbH, Switzerland). Three

replicates of each measurement was carried out and the average taken. The percentage attrition was calculated for the CGAC adsorbent was determined based on eqn. 1 :

$$\text{Loss on Attr. (\%)} = \frac{\text{Initial wt. of adsorbent} - \text{Wt. of adsorbent retained (g)}}{\text{Initial adsorbent weight (g)}} \times 100 \quad (1)$$

### 2.3 Batch sorption experiments

The working solutions for individual sorption experiments were prepared by serial dilution of aliquots of each stock solution. Batch sorption experiments for the equilibrium adsorption of Cd(II) and Pb(II) ions using the CGAC adsorbent was carried out by agitating known weight of the CGAC adsorbent with 100 mL of adsorbate solutions of different initial concentrations (50, 100, 150, 200, 250, 300, 350, 400, 450 and 500mgL<sup>-1</sup>). The pH 7 was used for the equilibrium, kinetics and adsorption studies investigating the effect of adsorbent dose and the pH for each experiment was modified using NaOH and HCl. The amount of adsorbent used was 2.0 g for the equilibrium and kinetics studies. The effect of contact time on the sorption processes was studied using 5 minutes to 180 minutes intervals. The reaction vessel for each adsorption experiment was a 250 mL conical flask and the sorption was carried out at a laboratory temperature of 25°C. Each conical flask with the adsorbate and adsorbent was agitated for a specified contact time in a Heidolph MR 3001 magnetic stirrer with speed and temperature controls at a speed of 200 rpm. At the end of each experiment, the resulting solution was separated from the adsorbent using Whatman (541) filter paper (Whatman International, England) and the filtrate analysed by taking out 5mL of each filtrate using a Volac high precision micropipette (Poulten & Graf GmbH, Germany) and diluting it to 50mL with deionized H<sub>2</sub>O. Thereafter, 10mL of the resulting metal ion solution was taken out using a micropipette into a sample analysis tube for metal ion determination. The metal ion concentrations of the adsorbate solution were determined using ICP-OES.

For the determination of metal ion loading after sorption, the amount of metal ion adsorbed at time t was calculated using eqn. 2.

$$qe = \frac{(C_i - C_t)V}{m} \quad (2)$$

Where  $C_t$  ( $\text{mgL}^{-1}$ ) is the metal ion concentration at time  $t$ ,  $q_t$  ( $\text{mgg}^{-1}$ ) is the loading of the metal ion at time  $t$ ,  $C_i$  is the initial metal ion concentration,  $m$  is the mass of the adsorbent and  $V$  is the volume of the aqueous system.

### 2.3.1 Experimental quality evaluation

All adsorption experiments were carried out in triplicates to ensure reproducibility and accuracy of results. The relative standard deviation was used as the error parameter for all analysis and the value for each set of measurements was  $< 5\%$ . Each experimental set was carried out using blanks to ensure the elimination of errors associated with experimental conditions. For each experimental analysis procedure, blanks were prepared using deionized water and the blank samples were subjected to the same treatment process using the same type of experimental vessel. In the analysis of Cd(II) and Pb(II) ions in solution, the blank samples were also analysed first in the Inductively coupled plasma optical emission spectrometer (ICP-OES)-Vista-MPX instrument prior to analysis of the standards and the samples. A calibration curve for each set of measurements was prepared by the ICP-OES software using the standards prepared for the Cd(II) and Pb(II) ions.

## 2.4 Theoretical models for fitting experimental data

### 2.4.1 Equilibrium isotherm models

Equilibrium modelling or adsorption isotherms have been studied to characterise the equilibrium sorption in a number of gas liquid and liquid-solid systems. In a liquid–solid adsorption system, the interaction between the adsorbent and the adsorbate is a dynamic process and the quantification of the effect of the adsorbent on the adsorbate system is determined by the amount of adsorbate that is removed by the adsorbent within specific conditions such as time, temperature, pH and amount of adsorbent. Thus, to have an understanding of the equilibrium description of the equilibrium relationship between these two phases that constitutes the adsorption system. The description of this interaction is often represented by equilibrium isotherm equations and these equations are used to characterise the relationship between the amount of substance adsorbed on the adsorbent and the amount of adsorbate remaining in solution (Athar *et al.*, 2013; El-Ashtoukhy *et al.*, 2008). The adsorption equilibrium data indicates the relationship between the mass of the adsorbate sorbed per unit mass of adsorbent ( $q_e$ ) and the adsorbate concentration for the solution at equilibrium  $C_e$  (Sarada *et al.*, 2014). Two

equilibrium isotherm models were used to characterise the removal of Cd(II) and ion from aqueous solution using the CGAC adsorbent and these were the Langmuir and Freundlich isotherms.

### *Langmuir Isotherm*

The Langmuir isotherm is a common model that has been used for the description of equilibrium sorption processes in literature. A basic assumption of the Langmuir isotherm is that sorption takes place at specific sites, which are uniformly distributed across the surface of the adsorbent (Langmuir, 1918; Basha *et al.*, 2009; Asuquo and Martin, 2016). The model can be written in its non-linear format as eqn.3:

$$q_e = \frac{q_m K_L C_e}{1 + K_L C_e} \quad (3)$$

Where  $q_e$  is the equilibrium metal ion concentration on the adsorbent ( $\text{mgg}^{-1}$ ),

$C_e$  is the equilibrium metal ion concentration in the solution ( $\text{mg}^{-1}$ ),

$q_m$  is the monolayer adsorption capacity of the adsorbent ( $\text{mgg}^{-1}$ ) also known as  $q_{\text{max}}$

$K_L$  is the Langmuir adsorption constant ( $\text{lmg}^{-1}$ ) related with the free energy of adsorption (Sari *et al.*, 2008).

### *Freundlich Isotherm*

The Freundlich isotherm assumes a heterogeneous adsorption surface and active sites with different energy based on multilayer adsorption. The model estimates the adsorption intensity of the adsorbate on an adsorbent (Freundlich, 1906; Athar *et al.*, 2013). The model in its non-linear form is given as eqn. 4:

$$q_e = K_F (C_e)^{1/n} \quad (4)$$

Where  $K_F$  is a constant relating to the adsorption capacity ( $\text{mgg}^{-1}$ )

$C_e$  is the concentration of metal ions at equilibrium ( $\text{mg}^{-1}$ )

$1/n$  is an empirical parameter relating to the adsorption intensity which varies with the heterogeneity of the material (Sari *et al.*, 2008; Asuquo and Martin, 2016).

## 2.4.2 Kinetic models

The kinetics of metal ion sorption processes in a batch system is also used to determine the type of processes that govern the mechanism of sorption. Kinetic data for metal ion sorption can be used to determine the type of mechanism governing the process and also the potential rate controlling step of the adsorption process. The mechanism of an adsorption process depends on the physical and chemical characteristics of the adsorbent as well as the mass transfer process from the adsorbate onto the adsorbent (Kumar *et al.*, 2010; Kumar *et al.*, 2014). Hence the discrimination of an adsorption mechanism may often involve the use of kinetic models that ascertain the mechanism governing the metal ion sorption based on shapes and fitting of kinetic plots which have fundamental assumptions in their design that can be extrapolated to the system under investigation. The information from the kinetic modelling can be used to interpret the type of transport mechanism and the description of the sorption process can therefore be carried out (Farooq *et al.*, 2011; Kakalanga *et al.*, 2012; Perez-Marín *et al.*, 2007). In this study, two adsorption reaction kinetic models {pseudo-first order (PFO) and pseudo-second order (PSO)} and one adsorption diffusion model (intraparticle diffusion) were applied to investigate the kinetics of Cd(II) and Pb(II) ion adsorption onto the CGAC adsorbent.

### Pseudo first order model

In 1898, Lagergren presented the first order rate equation for the adsorption of oxalic acid and malonic acid onto charcoal to explain the kinetics of adsorption on solid surfaces. In order to distinguish the kinetic processes based on concentration of solution and adsorption capacity of solid, this Lagergren equation is called the pseudo-first order equation (Lagergren, 1898; Ho, 2004a) was the first rate equation developed for sorption in liquid/solid systems and it is based on solid capacity (Ho, *et al.*, 2004). It is one of the most widely used rate equations reported in adsorption kinetic literature. Assuming that in a solid liquid adsorption system, the adsorption rate was proportional to the number of effective adsorption sites and then the rate of adsorption would be expressed as eqn (5):

$$\frac{dq_t}{dt} = K_1(q_e - q_t) \quad (5)$$

where  $q_e$  and  $q_t$  are the sorption capacities, at equilibrium and at time  $t$ , respectively ( $\text{mg}\cdot\text{g}^{-1}$ ), while  $K_1$  is the rate constant of the pseudo-first order sorption ( $\text{l}\cdot\text{min}^{-1}$ ). After integration and

applying boundary conditions  $t = 0$  to  $t = t$  and  $q_t = 0$  to  $q_t = q_t$ , the integrated form of eqn (6) is expressed as:

$$\log(q_e - q_t) = \log(q_e) - \frac{k_1}{2.303} t \quad (6)$$

Equation 7 is the linear form of the equation and the most common form of the pseudo first order (PFO) equation reported in literature for the description of sorption. Xuan *et al.*, (2006) used the linear pseudo first order equation to describe the kinetics of Pb(II) biosorption onto pre-treated chemically modified orange peel. Ho *et al.*, (2004) has also reported on the sorption of Pb(II) from aqueous solutions using tree fern adsorbent in which the linear form of the PFO equation was used. However, a number of studies have reported that the linear form of the PFO equation may lead to error propagation in the results due to the transformation of the PFO equation which is in a non-linear form to a linear form thereby implicitly altering the error structure in the determination of the model parameters (Ho, 2004b; Lin and Wang, 2009). The non-linear form of the PFO is given as eqn (7) as:

$$q_t = q_e(1 - e^{-k_1 t}) \quad (7)$$

The non-linear form of the PFO will be used to model the kinetics of sorption of Cd(II) onto the CGAC adsorbent used in this study and eqn.7 represents the reversible interaction between the adsorbate and adsorbent and is used for the prediction of the physisorption of the adsorbates onto the adsorbents in the system under consideration.

### Pseudo second order model

The reaction kinetics of adsorption is the basis of the adsorption reaction models used in kinetic modelling and one of the most commonly used reaction models for the description of the kinetics of adsorption is the pseudo-second order model proposed by Y.S. Ho in Ho, (2006). This model was proposed in an attempt to present the equation that represents the adsorption of divalent metals onto sphagnum moss peat during agitation. An assumption was made that the process may be second-order and that sorption depends on the adsorption capacity of the adsorbent which is associated with the number of available active sites. This pseudo second order kinetics is presumed to proceed via chemisorption which involves valence forces through the sharing or exchange of electrons between the peat and the divalent metal ion as covalent forces (Ho, 2006). In the work of Ho (2006), the adsorbent used was peat which has a number of

polar functional groups and these include ketones, phenolic acids and aldehydes. These chemical species on the surface of the peat are active sites that can be interact via chemical bonding. These groups are therefore the sites for the cation exchange capacity of the peat. Based on the above process and according to Coleman *et al*, (1956), the peat–copper reaction may be represented in two different forms as shown in the eqns. 8 & 9:



where  $P^-$  and  $HP$  are polar sites on the peat surface.

Here the rate of the second order reaction may be dependent on the amount of the divalent metal ions on the surface of the peat at time “t” and the amount of the divalent metal ions adsorbed at equilibrium, the assumption is also may that the adsorption follows the Langmuir equation (Ho and McKay, 2000; Ho, 2006; Qiu *et al.*, 2009). Hence, the rate expressions for the adsorption according to Ho and McKay, (2000) can be described by eqns. (10) and (11) as:

$$\frac{d(P)_t}{dt} = K[(P)_0 - (P)t]^2 \quad (10)$$

or

$$\frac{d(HP)_t}{dt} = K[(HP)_0 - (HP)t]^2 \quad (11)$$

Where  $(P)_t$  and  $(HP)_t$  are the number of active sites occupied on the peat at time t, and  $(P)_0$  and  $(HP)_0$  are the number of equilibrium sites available on the peat. Therefore the driving force ( $q_e - q_t$ ) is proportional to the available fraction of active sites. Thus from the above, the kinetic rate equation can be written as follows (Ho and McKay, 2000; Ho and Chiang, 2001; Ho, 2006):

$$\frac{dq_t}{dt} = K_2(q_e - q_t)^2 \quad (12)$$

Where  $q_e$  and  $q_t$  are the sorption capacities at equilibrium and at time t, respectively ( $\text{mg g}^{-1}$ ) and  $K_2$  constant is the rate constant of the pseudo-second order sorption ( $\text{g mg}^{-1} \text{min}^{-1}$ ). For the boundary conditions  $t = 0$  to  $t = t$  and  $q_t = 0$  to  $q_t = q_t$ , the integrated form of eqn. (12) becomes (Ho and McKay, 2000):

$$\frac{1}{qe-qt} = \frac{1}{qe} + K_2 \cdot t \quad (13)$$

This is the integrated rate law for a pseudo-second order reaction. Eqn. (13) can be rearranged to obtain:

$$q_t = \frac{t}{\frac{1}{k_2 q_e^2} + \frac{t}{q_e}} \quad (14)$$

Eqn (14) has the linear form:

$$\frac{t}{qt} = \frac{1}{K_2 qe^2} + \frac{1}{qe} t \quad (15)$$

Where  $h$  ( $\text{mg} \cdot \text{g}^{-1} \cdot \text{min}^{-1}$ ) can be regarded as initial sorption rate as  $q_t/t \rightarrow 0$ , hence:

$$h = K_2 \cdot qe^2 \quad (16)$$

Equation (16) can be written as:

$$\frac{t}{qt} = \frac{1}{h} + \frac{1}{qe} t \quad (17)$$

Equation (17) is the linear form of the pseudo second order equation (PSO) that is commonly reported in literature. This linear form causes distortion in the error structure when used to plot the PSO model leads to differences in model data between the non-linear and linear techniques in modelling the pseudo second order equation (Ho, 2004b; El-Khaiary *et al.*, 2010). Hence, the better option is the use of the non-linear method as the pseudo second order equation is a non-linear equation and the numerical optimization used to determine parameters will provide a more accurate representation of the model and the parameters within it than a linearization plot which often leads to propagation of errors in a model, (El-Khaiary *et al.*, 2010). This non-linear approach will be applied for the modelling of the sorption kinetics of Cd(II) and Pb(II) ions sorption onto the CGAC adsorbent and the non-linear PSO equation that will be used for the kinetic modelling is given by Lin and Wang, (2009) in eqn. 18 as :

$$q_t = \frac{K_2 \cdot qe^2 t}{1 + K_2 qe t} \quad (18)$$

Thus, equation (18) will be used to model the non-linear pseudo second order kinetics for the sorption reported in this work and it assumes a stronger interaction between the adsorbate and adsorbent based on the chemisorption of the adsorbates onto the adsorbents in the system under consideration. One advantage of using the pseudo second order equation for the modelling of adsorption kinetics is that there is no need to know the equilibrium capacity from the experiments, as this value, the pseudo second order rate constant and the initial adsorption rate can be calculated from the model (Ho, 2006).

#### *Intraparticle diffusion kinetic modelling*

Diffusion mass transport models have been applied to sorption systems and their role in pollutant sorption is extremely important. Generally, the adsorption process description using these diffusion models are usually based on one or more of the following, mechanistic steps:

- Diffusion of the solute from the solution to the film surrounding the particle.
- Diffusion from the film to the particle surface (external diffusion),
- Diffusion from the film to the internal sites (surface or pore diffusion)
- Metal ion uptake which can involve several mechanisms (adsorption and complexation)

The Weber and Morris intraparticle diffusion model is based on the assumption that the adsorption process may be controlled either by one of the following steps such as; film diffusion, pore diffusion, surface diffusion and adsorption onto the adsorbent pore surface or a combination of more than one step (Weber and Morris, 1963; Fierro *et al.*, 2008). These regimes can be obtained in a stirred batch system, wherein the diffusive mass transfer can be related by an apparent diffusion coefficient, which fits into an experimental sorption rate data (Fierro *et al.*, 2008). The intraparticle diffusion model assumes that in batch adsorption process, the adsorbate diffuse into the interior of the adsorbent and this process is dependent on the square root of time ( $t^{1/2}$ ) rather than time ( $t$ ), where the intercept ( $C$ ) is related to the boundary layer (Azarudeen *et al.*, 2015; Qiu *et al.*, 2009; Gurses *et al.*, 2014; Alkan *et al.*, 2007). The relationship for the model is given as follows:

$$q_t = K_{id}t^{1/2} + C \quad (19)$$

Where  $q_t$  is the amount of ions adsorbed at time  $t$  ( $\text{mgg}^{-1}$ ),  $K_{id}$  is the intraparticle diffusion constant ( $\text{mgg}^{-1}\text{min}^{-1/2}$ ) and  $C$  is the constant related to the thickness of the boundary layer

(Ahmadi *et al.*, 2015). A plot of  $qt$  vs  $t^{1/2}$  gives a straight line if intraparticle diffusion is the rate limiting step in the adsorption.

### 2.4.3 Data Analysis and Error Functions

The experimental equilibrium and kinetic data for the sorption of Cd(II) and Pb(II) ions onto the CGAC adsorbent were modelled using the equilibrium and kinetic models described in this study. To determine the model which best describes the sorption a number of fitting parameters were used to correlate the experimental data based on the magnitude of the correlation coefficient for the regression, that is the model which gives an  $r^2$  value closest to unity is deemed the best fit (Gimbert *et al.*, 2008; Hossain *et al.*, 2013). The fitting of these models with experimental data have been reported in a number of studies using a linearization of the different equilibrium and kinetic models for the sorption of various adsorbates onto different adsorbents (Ibrahim *et al.*, 2010; Gurses *et al.* 2014; Kumar *et al.*, 2014). However, this approach has been observed to be limited as it has an inherent bias resulting from the linearization approach as such data transformations implicitly alters the error structure and may result in a violation of the error equality of variance and normality hypotheses for standard least squares (Myers, 1990; Ratkowski, 1990; Gimbert *et al.*, 2008; Wong *et al.*, 2004). The use of non-linear optimization has been reported as a better approach for determination of model fitting to experimental data and the determination of isotherm parameter values as it most commonly uses algorithms for the determination of the parameters (Gimbert *et al.*, 2008; Wong *et al.*, 2004; Osmari *et al.*, 2013; Cassol *et al.*, 2014; El-Khaiary, 2008). The utilization of the non-linear approach requires the definition of error function to enable the optimization process to determine and evaluate the fitting of the models to the experimental data (Gimbert *et al.*, 2008). For the characterisation of the equilibrium and kinetic models for the sorption of Cd(II) and Pb(II) ions using the CGAC adsorbent, three different error parameters and the coefficient of determination( $r^2$ ) were determined using the solver add-in in Microsoft excel 2010 software.

These error functions are:

1- The Chi-square test ( $\chi^2$ )

$$\chi^2 = \sum_{n=1}^n \left( \frac{(q_{e,exp.n} - q_{e,model.n})^2}{(q_{e,exp.n})} \right) \quad (20)$$

2-The root mean square error (RMSE)

$$RMSE = \sqrt{\frac{1}{m-p} \sum_{i=1}^m (qm - qe)^2} \quad (21)$$

3- The coefficient of determination ( $r^2$ )

$$r^2 = \frac{\sum (qe_{model} - qe_{av.})^2}{\sum (qe_{model} - qe_{av.})^2 + \sum (qe_{model} - qe_{exp.})^2} \quad (22)$$

Where:  $qe_{model}$  is the equilibrium capacity obtained from the isotherm model

$qe_{exp.}$  is the equilibrium capacity obtained from experiment

$qe_{av.}$  is the average  $qe_{exp.}$

$qe$  and  $qm$  are the measured and model amount of cadmium(II) ion adsorbed at time  $t$  respectively

$m$  is the number of data points evaluated

$p$  is the number of parameters in the regression model

Whereby the smaller the values of the error parameters (RMSE and  $\chi^2$ ) and the higher the  $r^2$  value indicates a better fitting of model with the experimental data (Basha *et al.*, 2009).

### 3. Results and discussions

#### 3.1 Adsorbent characterisation

The commercial activated carbon (CGAC) adsorbent was characterised to determine its surface area and porosity, surface morphology, chemical composition, functional groups present, loss on attrition, pH and pH<sub>pzc</sub> based on the methodology reported in the experimental section of this work. Some of the results obtained from this characterisation are presented in Table 1. The surface area of the CGAC adsorbent and the pore size distribution obtained from the characterisation is presented in Fig. 1. Fig. 1 and results from Table 1 indicates that the activated carbon has a very high BET surface area of 4273 m<sup>2</sup> g<sup>-1</sup>. This was expected of a commercial prepared activated carbon. The pore size of an adsorbent is an important parameter in the characterisation of porous materials as it gives information on the structural heterogeneity of a porous material.

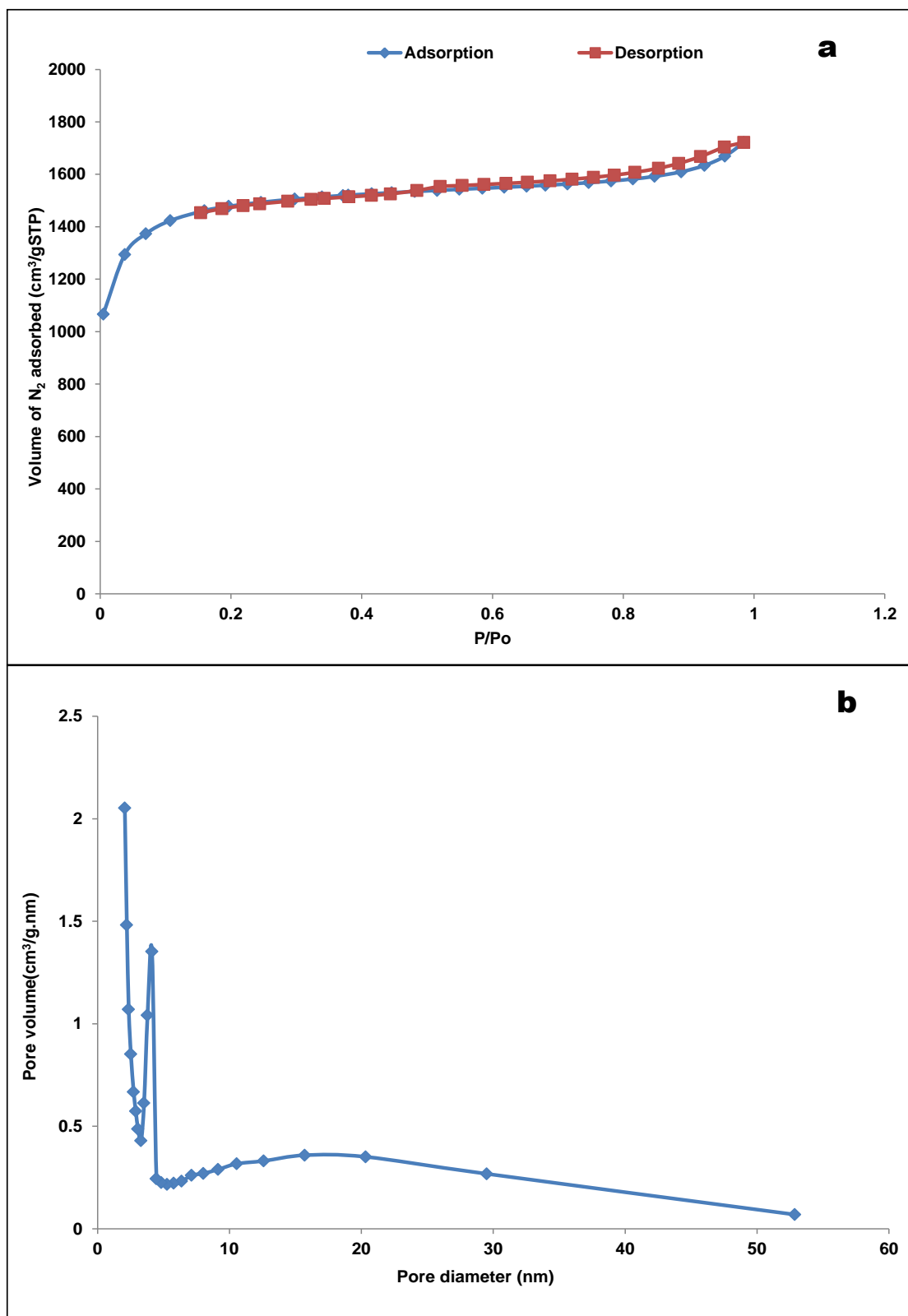


Figure 1: N<sub>2</sub> adsorption-desorption isotherm (a) and pore size distribution (b) of CGAC

From this analysis, it was observed that the average pore diameter of the CGAC adsorbent was 4.48 nm, with a total pore volume of 2.66 cm<sup>3</sup> g<sup>-1</sup>. The CGAC adsorbent was observed to exhibit a narrow bimodal pore size distribution between 3-12nm, while a wider distribution is observed

from 15-52nm as can be observed in Fig. 1. The BET surface area of the CGAC adsorbent was higher than what has been reported for some commercial activated carbon in literature. Al-Lagtah *et al.*, (2016) has reported on the characterisation of two commercial activated carbons, CAC1-commercially known as DARCO 12X20 and CAC2-commercially known as NORIT GAC 1240W. According to the study, the BET surface area of these two adsorbents were; 643  $\text{m}^2 \text{g}^{-1}$  (CAC1) and 902  $\text{m}^2 \text{g}^{-1}$  (CAC2). The total pore volume for the CGAC adsorbent was also observed to be higher than what has been reported by Al-Lagtah *et al.*, (2016) for the two commercial activated carbons, these were; 0.53  $\text{cm}^3 \text{g}^{-1}$  for CAC1 and 0.64  $\text{cm}^3 \text{g}^{-1}$  for CAC2. Similarly, the average pore size of the CGAC adsorbent was higher than what was reported for the CAC1 and CAC2 adsorbents which were 1.64 and 1.50 nm respectively (Al-Lagtah *et al.*, 2016). Mailler *et al.*, (2016) has also reported on the BET surface area and pore characteristics of some commercial activated carbon adsorbents used in the adsorption of micropollutants in wastewater. In their study, the BET surface area of the activated carbons were all observed to be lower than that of the CGAC adsorbents and these were; PB170-DaCarb (957  $\text{m}^2 \text{g}^{-1}$ ), WP 235-Chemviron (909  $\text{m}^2 \text{g}^{-1}$ ), W35-Norit (768  $\text{m}^2 \text{g}^{-1}$ ) and PC1000-DaCarb (458  $\text{m}^2 \text{g}^{-1}$ ). The pore volumes of these adsorbents were; 0.50  $\text{cm}^3 \text{g}^{-1}$ (PB170), 0.48  $\text{cm}^3 \text{g}^{-1}$  (WP235), 0.49  $\text{cm}^3 \text{g}^{-1}$ (W35) and 0.24  $\text{cm}^3 \text{g}^{-1}$ (PC1000) and these were all lower than that of the CGAC adsorbent.

Table 1: Characteristics of CGAC adsorbent

Parameter	Value
BET surface area ( $\text{m}^2 \text{g}^{-1}$ )	4273
Total Pore volume ( $\text{cm}^3 \text{g}^{-1}$ )	2.66
Micropore volume ( $\text{cm}^3 \text{g}^{-1}$ )	2.04
Mesopore volume ( $\text{cm}^3 \text{g}^{-1}$ )	0.62
Micropore area ( $\text{m}^2 \text{g}^{-1}$ )	3697
Percent of micropores (%)	76.64
Percent of mesopores (%)	23.35
BJH desorption average pore diameter (nm)	4.48
Bulk density( $\text{g cm}^{-3}$ )	0.69
Loss on attrition (%)	4.10
pH	7.80
pHpzc	7.20

The adsorption process in porous materials such as activated carbon type materials takes place in the pores of the adsorbent. The size of the pores in an adsorbent affects the type of transport mechanism or activity that takes place on the adsorbent surface. The classifications of these pores are as follows (Sing, 1982):

1. Micropores (pore size < 2 nm),
2. Mesopores (2 nm ≤ pore size ≤ 50 nm),
3. Macropores (pore size > 50 nm)

Based on the N<sub>2</sub> adsorption-desorption isotherm which indicates a type IV adsorption isotherm and the pore size (4.88nm), the CGAC adsorbent can be classified as a mesoporous adsorbent. The shape of the CGAC adsorbent N<sub>2</sub> adsorption-desorption isotherm (Fig. 1) can also be used to determine what type of hysteresis is present during N<sub>2</sub> adsorption-desorption. From Fig. 1, it was observed that the curve indicates the presence of H1 type hysteresis loop which is often present in adsorbents with narrow distribution of pore sizes (Naumov, 2009).

The total pore volume of an adsorbent is also used as a measure of adsorption loading since its measurement is based on the amount of adsorbate (liquid nitrogen) adsorbed (Tsai *et al.*, 2001). The pore volume of an adsorbent is used to give characteristic information on the ability of the material to adsorb molecules which can be extrapolated to liquid systems. Hence its utilisation as a parameter in the characterisation of carbon based adsorbents used in aqueous systems. The high pore volume of the CGAC adsorbent indicates that it has substantial pores to adsorb adsorbates. The bulk density of an activated carbon adsorbent is a characteristic that is determined by the nature of the precursor and the degree of treatment the precursor was subjected to for the manufacture of the adsorbent (Acharya *et al.*, 2009). It is used to determine the volume capacity of an activated carbon, which in turn can be used to determine the working capacity of an adsorber (Al-Lagtah *et al.*, 2016). The bulk density of the CGAC adsorbent was 0.69 g cm<sup>-3</sup> which is typical for granular activated carbons (Harsh and Rodriguez-Reinoso, 2006). This value was observed to be higher than those reported by Mailler *et al.*, (2016) for some commercial activated carbon adsorbents which were; 0.30g cm<sup>-3</sup> (PB170), 0.38g cm<sup>-3</sup> (WP235), 0.33g cm<sup>-3</sup> (W35) and 0.54g cm<sup>-3</sup> (PC1000) and these adsorbents were obtained from wood, coal, peat and coconut precursors respectively. Similarly, the bulk density of the CGAC adsorbent was higher than those of the CAC1 and CAC2 adsorbents reported by Al-Lagtah *et al.*, (2016) which were 0.38 g cm<sup>-3</sup> and 0.49 g cm<sup>-3</sup> respectively (Al-Lagtah *et al.*, 2016).

The characteristic of attrition resistance of adsorbents is important in the utilisation of adsorbents as it gives information on what type of reactor system can be most suited for an adsorbent. Adsorbents that have high resistance to attrition (low losses) such as the commercial activated carbon used in this study which had losses of 4.1% due to attrition (Table 1) can be used in agitated reactor systems where there is mixing. This gives this adsorbent considerable advantage over some other adsorbents that have high losses associated with attrition as this will make the material susceptible to the production of fine particles which can cause blockage in reactors.

### 3.1.1 pH and pHpzc of adsorbent

The zeta potential is a parameter that accounts for most surface phenomena such as agglomeration and deposition of particles as well as their stability (Alkan *et al.*, 2009). When an adsorbent is immersed into an aqueous system in a powdered or granular form and subjected to agitation as is the process in batch adsorption studies, the interaction of the adsorbent surface with the species in the aqueous solution or system depends on many factors which are governed by the type and number of species, pH of the aqueous system and the nature and type of potential or charge on the adsorbent surface. The zeta potential can be used to estimate the effects of the particle charge on adsorption and aggregation behaviour of ions with respect to the adsorbent. From the determination of the zeta potential of an adsorbent-aqueous system which is always carried out with respect to the aqueous system pH, a characteristic parameter can be obtained by plotting the zeta potentials at different pH as a function of pH. This plot indicates that as the pH of a solution moves from acidic to basic, a point is reached where the adsorbent-aqueous system has a pH at which there is an inflection from a positive surface (associated with positive zeta potential) to a negative surface (associated with a negative zeta potential). This point of inflection on the pH has a potential of zero and is described as the pH at which the point has a zero charge (pHpzc) and here the surface acidic (or basic) functional groups no longer contribute to the pH value of the aqueous system (Nomanbhany and Palanisamy, 2005). This pHpzc value is an important parameter as it gives information on the pH that can be used for adsorption of cations and anions; due to the understanding of the regions within the pH window that is dominated with basic or acidic functional groups (Fernandez *et al.*, 2015).

The results of the pH (7.8) and pHpzc (7.2) of the CGAC adsorbent are presented in Table 1. The results of the pH and pH point of zero charge (pHpzc) of the CGAC adsorbent indicates that the material is basic in nature and since the ions of interest for sorption studies are cations {Cd(II) and Pb(II)} the value of pH of 7 was chosen for use in adsorption studies for Cd(II) and Pb(II)

ion sorption. It can also be observed that the value of the pH of the adsorbent mixture can be closely associated with the pH<sub>pzc</sub>. The results for the pH and pH<sub>pzc</sub> of the CGAC adsorbent is similar to that observed by Al-Lagtah *et al.*, (2016) for two commercial activated carbon adsorbents- CAC1 and CAC2, which had values of pH (4.9 and 9.1) and pH<sub>pzc</sub> (4.8 and 9.0) respectively. Similarly, from these values, it can also be observed that the value of the pH can be closely associated with the pH<sub>pzc</sub> as observed by Al-Lagtah *et al.*, (2016).

### 3.1.2 Adsorbent Morphology

The morphology of the CGAC adsorbent before and after adsorption of Cd(II) and Pb(II) ions was determined using a scanning electron microscope. SEM micrographs enable the direct observation of changes to surface microstructures of carbons (Goel *et al.*, 2005). The SEM images of the commercial activated carbon (CGAC) with different magnifications before and after sorption of Cd(II) and Pb(II) ions are shown in Fig. 2-4. From the results, the surface of the CGAC is observed to have morphologies that are uneven and heterogeneous which may have important effect on the adsorption process (Ge *et al.*, 2016).

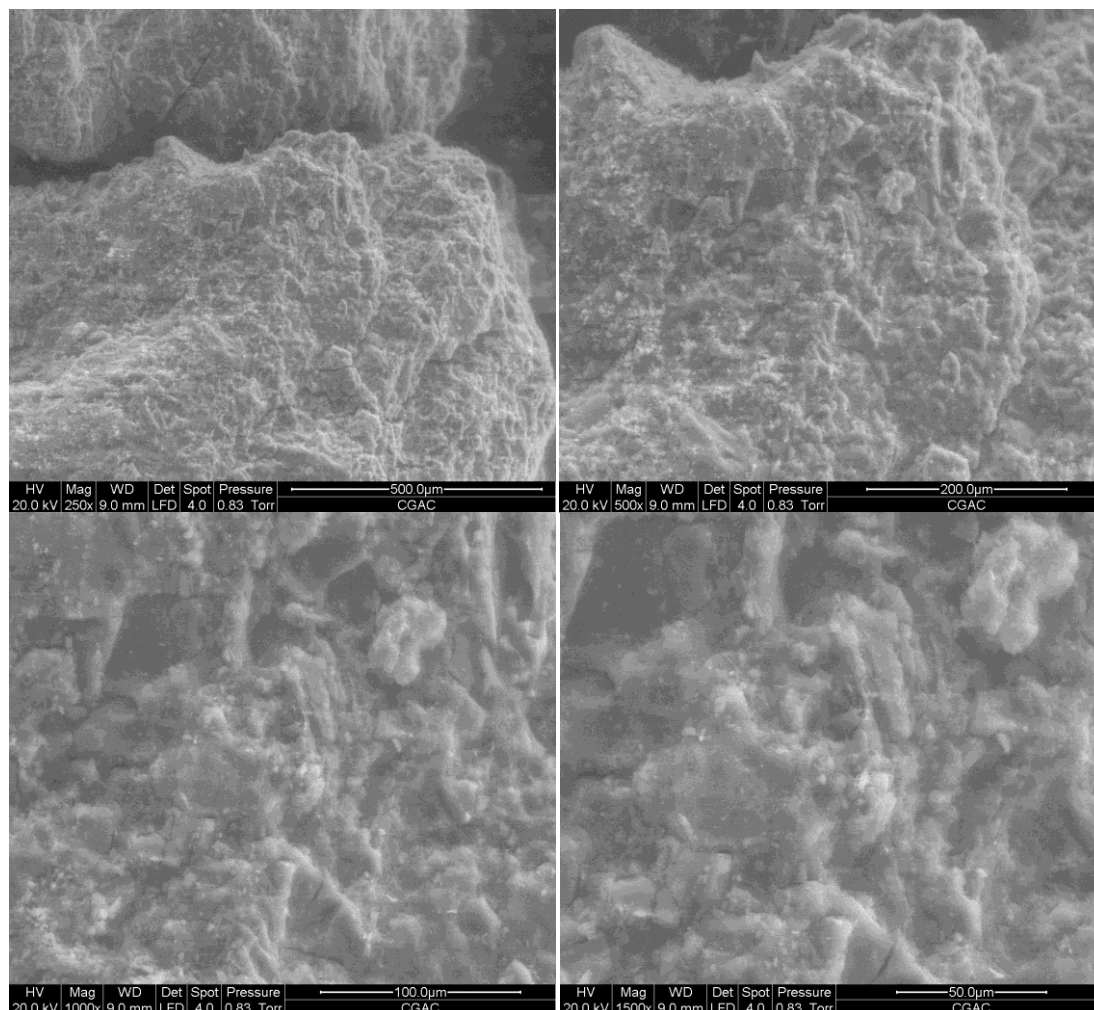


Figure 2: SEM micrograph of commercial activated carbon CGAC

The surface of the CGAC adsorbent was rough and coarse with irregular crevices with different dimensions that may indicate the presence of macro and meso pores which are probable sites for metal ion transport and sorption. A similar observation with respect to the presence of these cavities on the CGAC adsorbent has also been reported Anisuzzaman *et al.*, (2015) in their study on commercial activated carbon adsorbents modified for phenol removal. In addition, it was also observed that some of these pores were visible from the SEM images even though few macropores were observed as the adsorbent has higher amounts of mesopores based on the pore size distribution (Fig.1). Furthermore, the pore network in the CGAC adsorbent is presumed to originate due to the evolution of the volatile organic components of the precursor material during the thermal preparation and activation of the adsorbent (Tounsadi *et al.*, 2016).

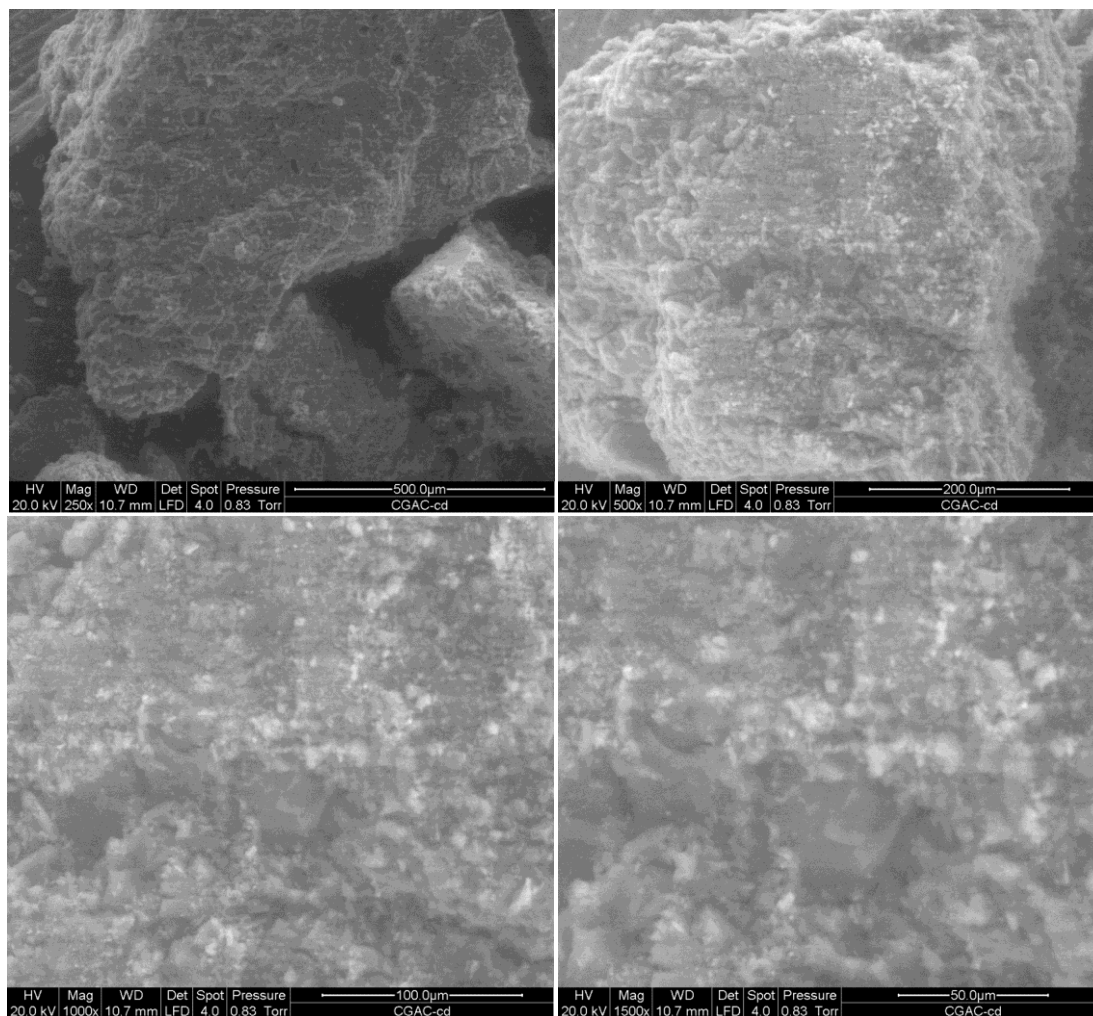


Figure 3: SEM micrograph of CGAC after Cd(II) sorption (CGAC-Cd)

The SEM micrographs also indicate the presence of corrugated surfaces with boundary edges on the CGAC adsorbent and these were still present in the micrographs of the CGAC adsorbent after metal ion sorption (Fig.3 and 4). The SEM images after metal ion adsorption also indicates the presence of crevices on the used adsorbents. Comparing the micrographs in Figs. 2-4, it can be observed that the surface of the adsorbent after Cd(II) (Fig. 3) and Pb(II) (Fig.4) sorption were more disaggregated with increased roughness. These surface alterations in the SEM of the spent adsorbents may be associated to the effect of the sorption processes on these adsorbents as the aqueous adsorbate system interacts with the adsorbent.

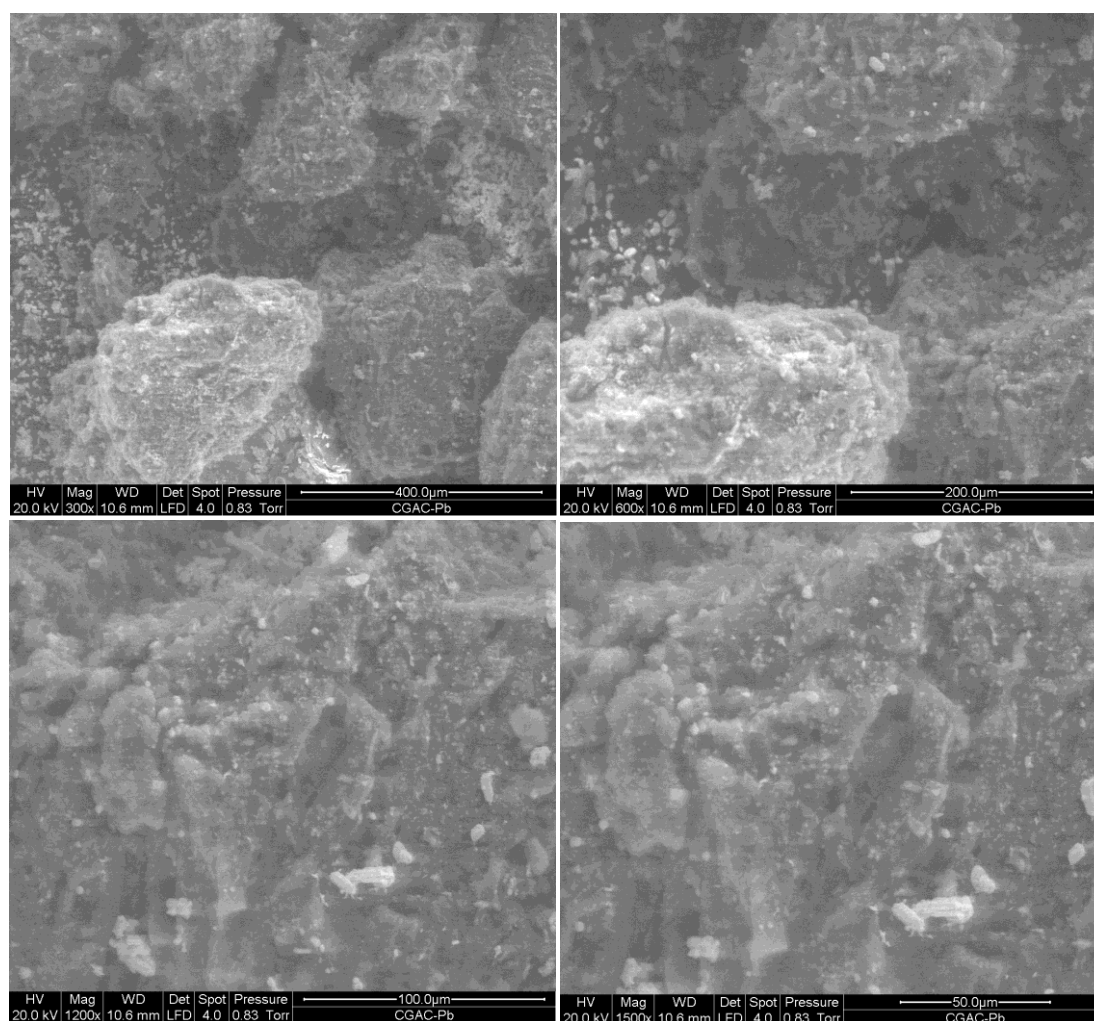


Figure 4: SEM micrograph of CGAC after Pb(II) sorption (CGAC-Pb)

It is presumed that during the batch sorption which occurred at constant agitation, the cavities on the CGAC adsorbent surface would serve as channels for the Cd(II) and Pb(II) ions in the adsorbate system, thereby providing access to the meso and micropores where surface adsorption and chemical interactions can occur with the surface functional groups on the adsorbent active sites (Pezoti *et al.*, 2016).

### 3.1.3 Adsorbent Chemical Composition

EDX analysis of the chemical composition of the CGAC adsorbent was also carried out and the spectrum of the of the CGAC adsorbent is shown in Fig. 5 and indicates that the commercial activated carbon adsorbents had a high carbon content (89%), an oxygen content of 5.5% and trace quantities of other heteroatoms such as aluminium, silicon, molybdenum and calcium. The chemical content of the CGAC adsorbent is observed to be similar to that of another commercial activated carbon adsorbent-CAC reported by Gupta *et al.*, (2012) in their study on mesoporous adsorbents for heavy metal removal. In their study, the carbon content of the CAC adsorbent obtained from EDX analysis was 89%, while the oxygen content was 10 %. It is pertinent to observed that both the CAC adsorbent reported by Gupta *et al.*, (2012) and the CGAC adsorbent examined in this study were obtained from the same manufacturer (Chemviron) and this may account for the similarity observed. The CGAC EDX spectra after metal ion sorption are shown in Fig. 6 for Cd(II) ion and Fig. 7 for Pb(II) ion sorption.

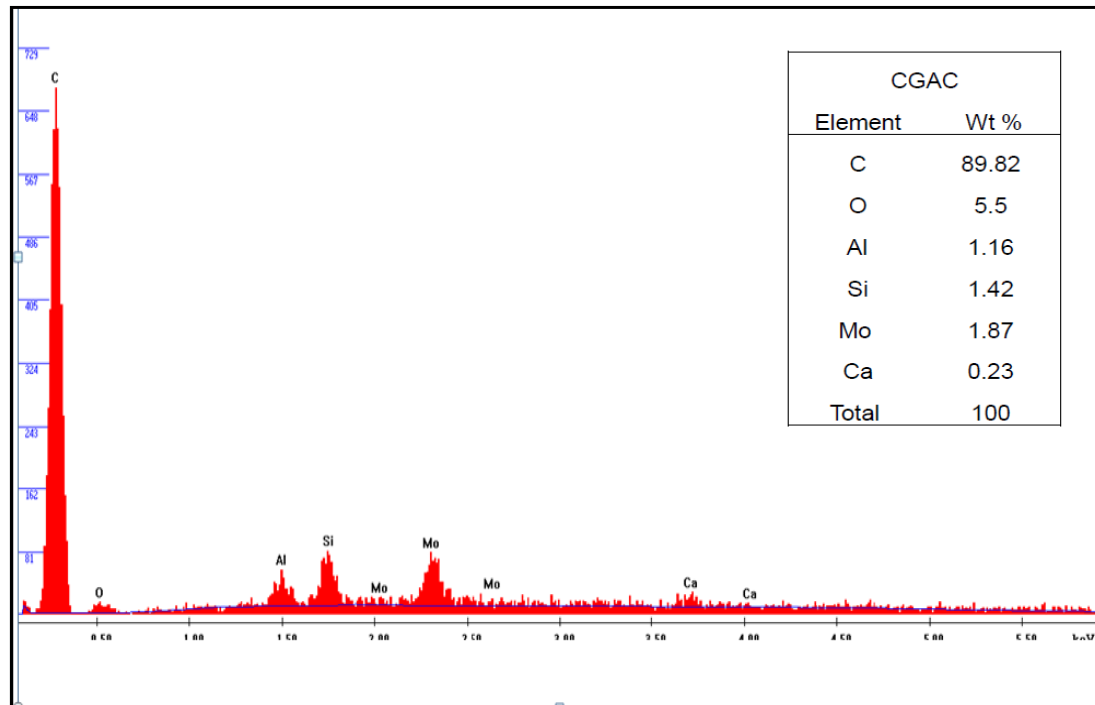


Figure 5: EDX spectrum of CGAC adsorbent

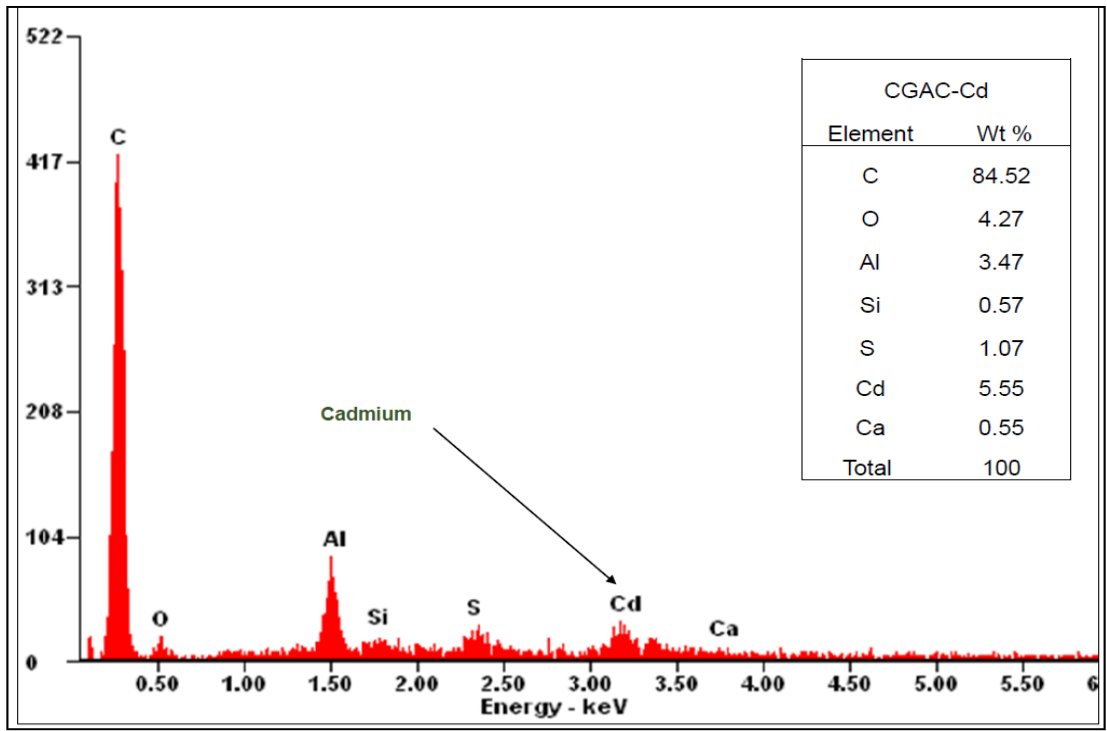


Figure 6: EDX spectrum of CGAC adsorbent after Cd adsorption (CGAC-Cd)

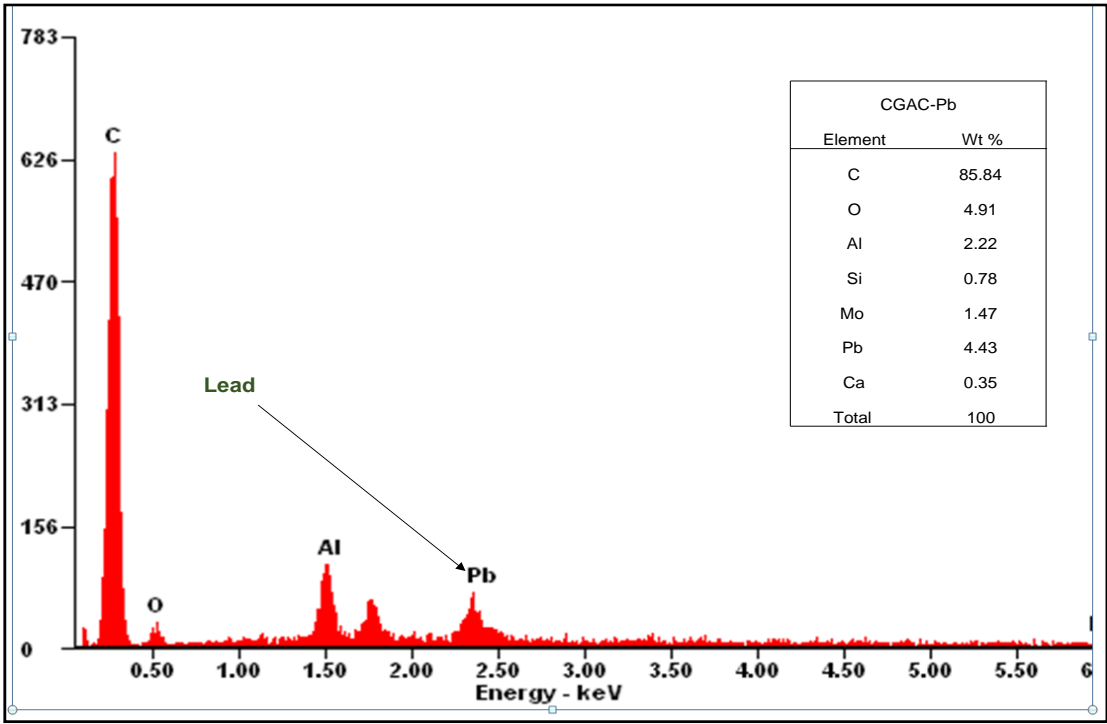


Figure 7: EDX spectrum of CGAC adsorbent after Pb adsorption (CGAC Pb)

From Figs. 6 and 7, the EDX spectrum for each sorption process shows corresponding peaks for the metal ions Cd(II) & Pb(II) confirming their existence on the surface of the activated carbon adsorbent after sorption was carried out. It is also pertinent to observe that the carbon and

oxygen content of these used CGAC adsorbents were lower than that of fresh adsorbent presented in Fig. 5. This may be associated to the effect of the washing and filtering step of the used adsorbent which may lead to the losses which can influence the composition of the adsorbent. In addition, this observation may also be related to the nature of the samples and spot size analysis carried out. The results of the EDX analysis of the CGAC adsorbent before and after Cd(II) and Pb(II) ion sorption lends credence to the observation that the CGAC adsorbent was able to remove these metal ions from their respective aqueous systems. This observation has also been reported by Erdem *et al.*, (2013) in their study on the accumulation of Pb(II) onto activated carbon derived from waste biomass, wherein the existence of Pb(II) ion peak on the EDX spectrum was used to prove the accumulation of the metal ion on the adsorbent. Gupta *et al.*, (2012) has also reported on the use of the EDX spectrum after Pb(II) and Ni(II) ion adsorption onto the surface of mesoporous carbon adsorbents to establish that the adsorption of the metal ions did take place.

#### 3.1.4 Thermogravimetric analysis

Thermogravimetric analysis is a thermal decomposition technique that quantifies the weight loss of a material as a function of temperature or time under controlled atmosphere. This degradation profile can provide information on the approximate chemical components such as moisture, fixed carbon and volatile components of materials due to the nature of their degradation with increasing temperature. It is also used to determine the temperature range within which a material acquires fixed chemical composition or which it decomposes (Pezoti *et al.*, 2016). Thermo-gravimetric analysis (TGA) of the CGAC adsorbent in Fig. 8 reveals two regions of weight loss- I and II. The first region (I) occurring approximately between 30-100°C is associated with weight loss due to the elimination of water molecules and this loss accounted for about 5.5%. The water molecules may either have been physically absorbed or hydrogen bonded onto the surface of the CGAC adsorbent (Li *et al.*, 2016; Ali *et al.*, 2016). The second weight loss region (II) occurring approximately between 110-590°C may be attributed to the decomposition and elimination of the volatile organic components that were still present on the CGAC adsorbent surface after the commercial manufacturing.

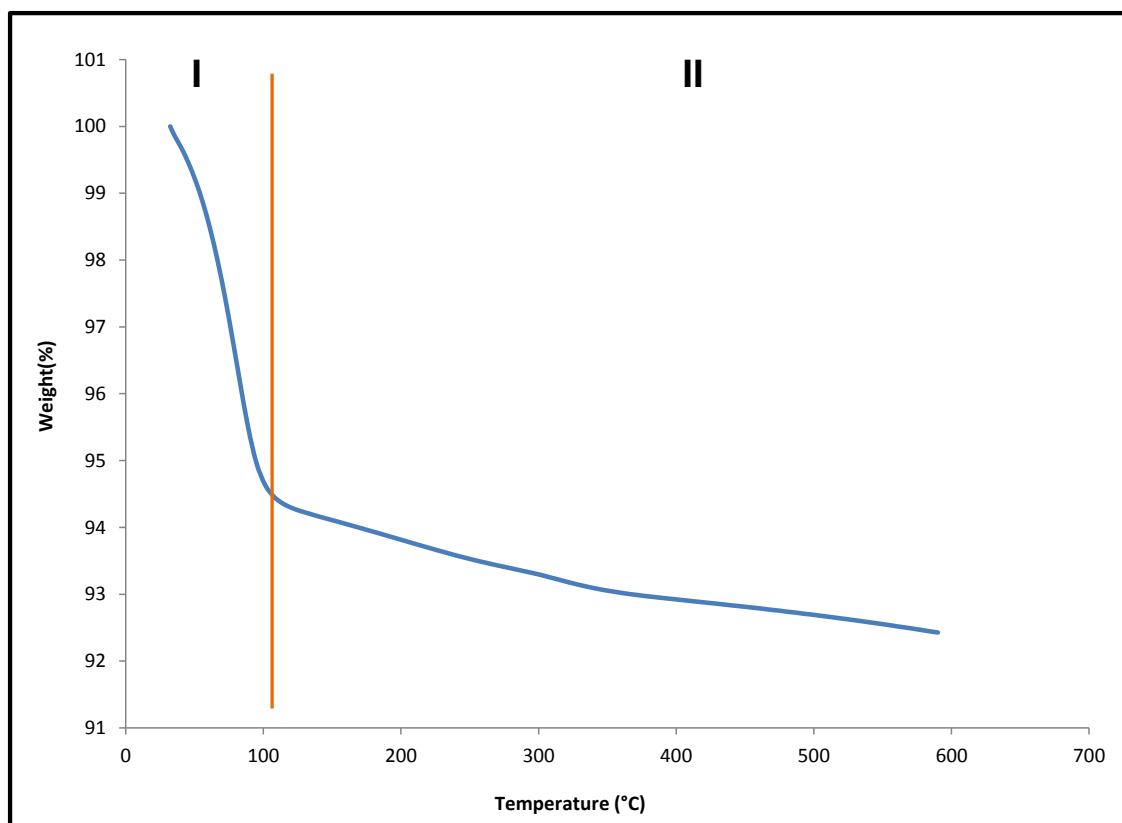


Figure 8: Thermogravimetric analysis of CGAC adsorbent under N<sub>2</sub>

This weight loss was about 2.1% and the total weight loss under thermal decomposition of the CGAC adsorbent was 7.6%. This indicates that the adsorbent was made up about 90% carbon that was stable under the thermal degradation. It also implies that the volatile components of the precursor material used to manufacture the activated carbon were completely eliminated from the surface of the activated carbon due to its high thermal stability. This observation of high thermal stability of activated carbon adsorbent under thermogravimetric analysis has also been observed by Pezoti *et al.*, (2016) in their study on the synthesis and characterisation of a NaOH-activated carbon adsorbents used for amoxicillin removal.

### 3.1.5 Fourier transform infrared (FTIR) spectroscopy

The presence of functional groups on an adsorbent's surface is important for adsorption and accordingly to Tansel and Nagarajan, (2004) the effectiveness of an activated carbon adsorbent used for the removal of specific contaminants is strongly dependent on the presence of functional groups on the carbon adsorbent surface. The types of functional groups on the CGAC adsorbent was determined using Fourier transform infrared (FTIR) spectroscopy. FT-IR spectra obtained for the CGAC adsorbent and after Cd(II) and Pb(II) ion sorption are presented in Figs. 9-11.

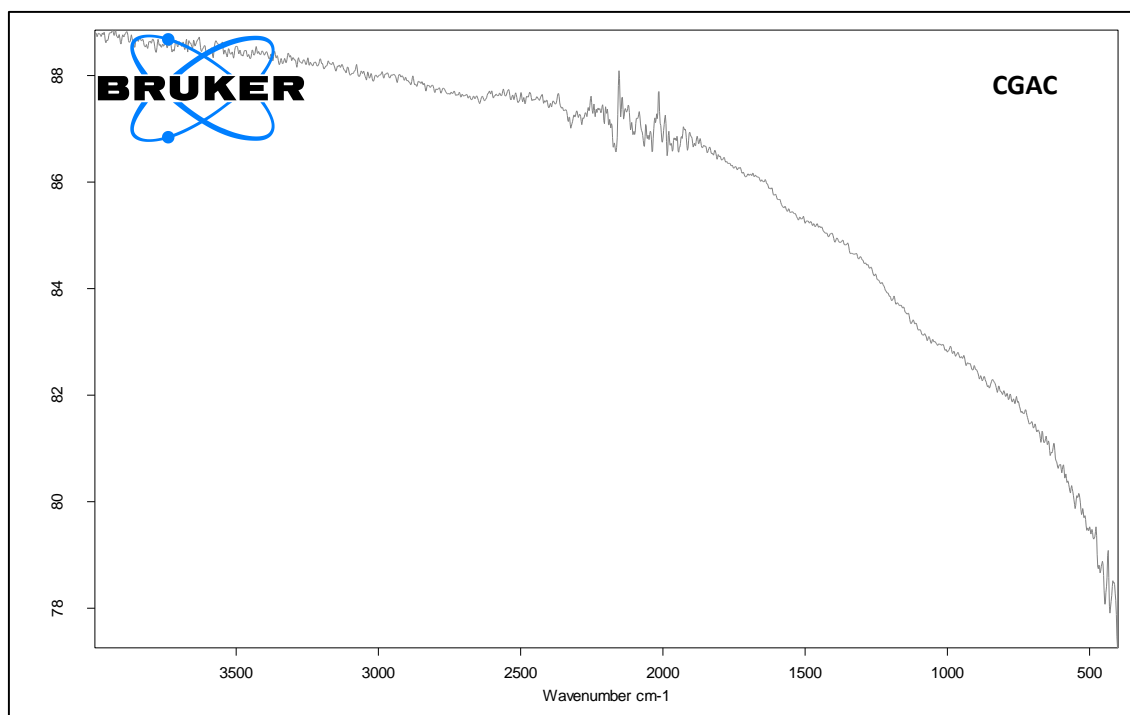


Figure 9: FTIR spectra of CGAC adsorbent

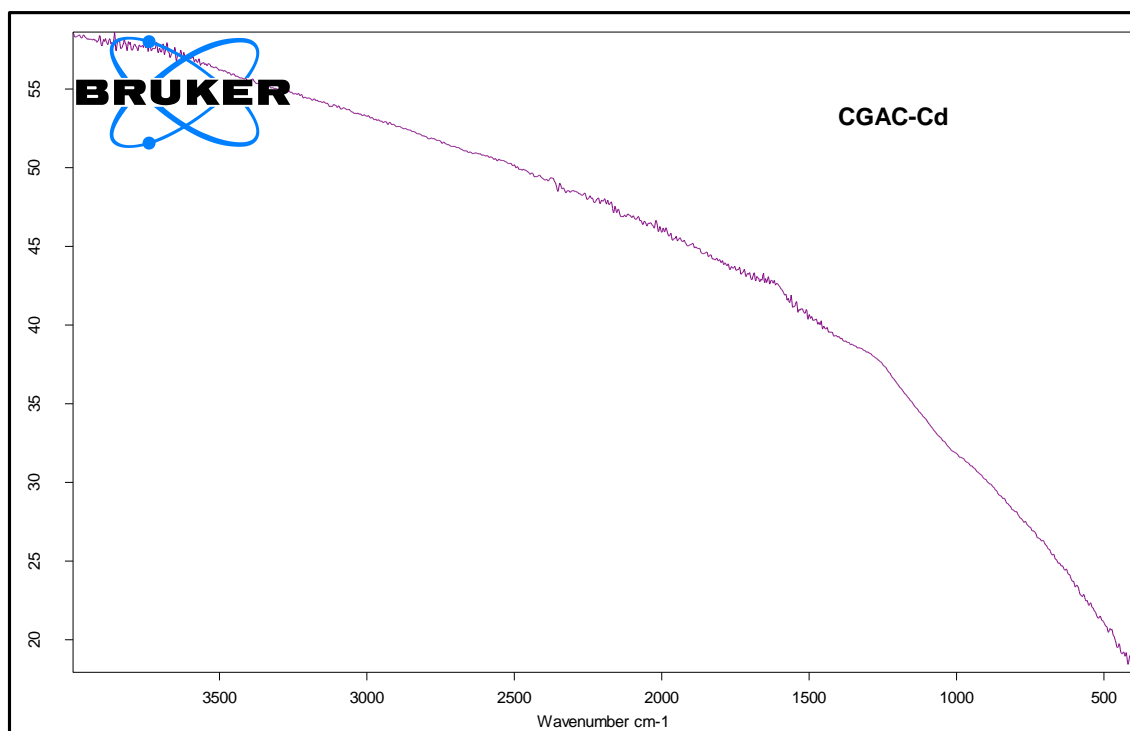


Figure 10: FTIR spectra of CGAC adsorbent after Cd(II) adsorption (CGAC-Cd)

From Figs. 9-11, it is observed that the peak intensity of the functional groups on the CGAC adsorbent were low. From the spectra of the CGAC adsorbent (Fig. 9), peaks were observed at 2368, 2155, 2083, 2013 and 455 $\text{cm}^{-1}$ . The peaks at 2368 $\text{cm}^{-1}$  and 2155 $\text{cm}^{-1}$  indicates the presence of (C $\equiv$ C) vibrations in the alkyne groups (Wang *et al.*, 2016; Kazemi *et al.*, 2016) that

can be related to the nature of the activated carbon precursor (coal). The peaks at 2083 and 2013 $\text{cm}^{-1}$  are characteristic of the  $\nu(\text{C}=\text{O})$  vibration (Jaouen and Salmain, 2015; Wang *et al.*, 2015) and may be associated with the presence of some co-ordinated carbonyl groups on the CGAC surface (Boag *et al.*, 2008). The peak at 455  $\text{cm}^{-1}$  can be assigned to the  $\gamma(\text{C}-\text{C})$  and  $\gamma(\text{C}-\text{H})$  vibrations that are commonly found in polycyclic aromatic hydrocarbon compounds (Agudelo-Castaneda *et al.*, 2015). This peak at 455 $\text{cm}^{-1}$  has also been reported to be a characteristic peak for the vibration of the Si-O-Si skeleton (Tsoncheva *et al.*, 2015), which may give insight into the nature of bonding of the silicon compounds identified in the EDX spectra of the CGAC adsorbent (Fig. 5).

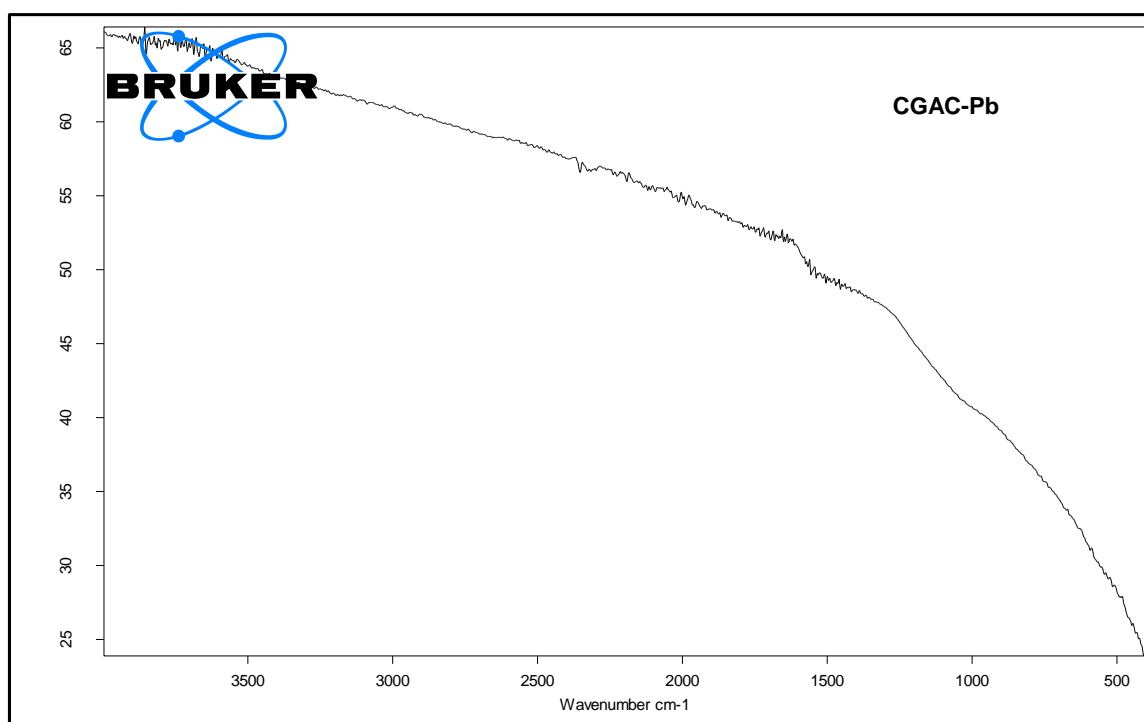


Figure 11: FTIR spectra of CGAC adsorbent after Pb(II) adsorption (CGAC-Pb)

The spectra of the CGAC adsorbent after Cd (II) and Pb (II) metal ion sorption are illustrated in Figs.10 – 11. Peak shift on the some of the vibrations after metal ion sorption can be seen these two figures. The  $\text{C}\equiv\text{C}$  peak at 2368 and 2155  $\text{cm}^{-1}$  for the CGAC adsorbent was observed at different wavenumbers after Cd (II) and Pb (II) adsorption, these peaks showed shift to 2318  $\text{cm}^{-1}$  and 2137 $\text{cm}^{-1}$  for Cd (II) ion (Fig. 10) and 3280  $\text{cm}^{-1}$ , while that for Pb(II) ion (Fig.11) were at 2346  $\text{cm}^{-1}$  and 2134 $\text{cm}^{-1}$  respectively. Furthermore, the  $\nu(\text{C}=\text{O})$  vibration observed for the CGAC adsorbent at 2083  $\text{cm}^{-1}$  was observed at 2073  $\text{cm}^{-1}$  after Cd(II) ion sorption and 2054  $\text{cm}^{-1}$  after Pb(II) ion adsorption. The spectra of the CGAC adsorbent after Cd(II) ion adsorption (CGAC-Cd) shown in Fig. 10 was also observed to indicate a new peak at 1550  $\text{cm}^{-1}$  that can be

associated with N-H bending deformations in amides and C=N stretching (amide II) and N=O asymmetric vibrations in nitro (NO<sub>2</sub>) groups (Bacsik *et al.*, 2011), this peak has also been associated with the asymmetric vibration of the O-C-O group (Sahoo *et al.*, 2012). The spectrum after Pb(II) ion sorption (CGAC-Pb) seen in Fig.11 showed the presence of a new peak at 1655 cm<sup>-1</sup> which can be assigned to the C=C and C=O stretching vibrations of the hydrocarbon and carbonyl moieties on the spent adsorbent surface (Bacsik *et al.*, 2011).

Based on the shifts in the peaks observed in the IR spectra obtained for the CGAC adsorbents, it can be inferred that some of the functional groups on the activated carbon such as carboxyl, amides, ethers, and cyano and nitro groups may be active sites for the Cd (II) and Pb (II) ion sorption from the adsorbate. The decrease in wavenumbers of some of these peaks in the spectra obtained after adsorption (Fig. 10 and 11) indicates that there may be interactions between the Cd(II) and Pb(II) ions and these functional groups during adsorption (Paduraru *et al.*, 2015; Chand *et al.*, 2014; Simonescu, 2012; Iqbal *et al.*, 2009a). The shift in vibrations of some of the functional groups after metal ion sorption as observed in this study can be explained based on the change in coordination sites of the functional groups due to the interactions with the Cd (II) and Pb (II) ions (Thirumavalavan *et al.*, 2011).

### 3.2 Adsorption Kinetics

The study of metal ion sorption kinetics can provide insight on the rate and mechanism of sorption as it gives information that can be used to understand the type of adsorbent-adsorbate interaction and the mechanism of adsorbate removal. Adsorption experiments to study the effect of contact time on the removal of cadmium (II) and lead (II) metal ions from aqueous solutions were carried out at pH 7 and a temperature of 25 °C using 500mgL<sup>-1</sup> metal ion concentration in a 100mL metal ion-adsorbent system at 200 rpm and the amount of adsorbent used was 2.0g. Sorption experiments were carried out for the following time intervals: 5, 10, 15, 20, 25, 30, 40, 60, 90, 120 and 180 minutes.

The kinetic profiles for the sorption of the two metal ions are presented in Fig. 12 and indicates that for both metal ions {Cd(II) and Pb(II)} sorption took place via two stages namely - a fast sorption uptake that occurred within 30minutes of sorbate-sorbent contact. This was followed by a slow phase of metal ion removal that developed from 40 minutes until 180 minutes when an equilibrium or quasi-stabilised state was presumed to have been reached. The metal ion loadings after 180 minutes were 17.23 mgg<sup>-1</sup> for Cd(II) ion and 16.84 mgg<sup>-1</sup> for Pb(II) ion.

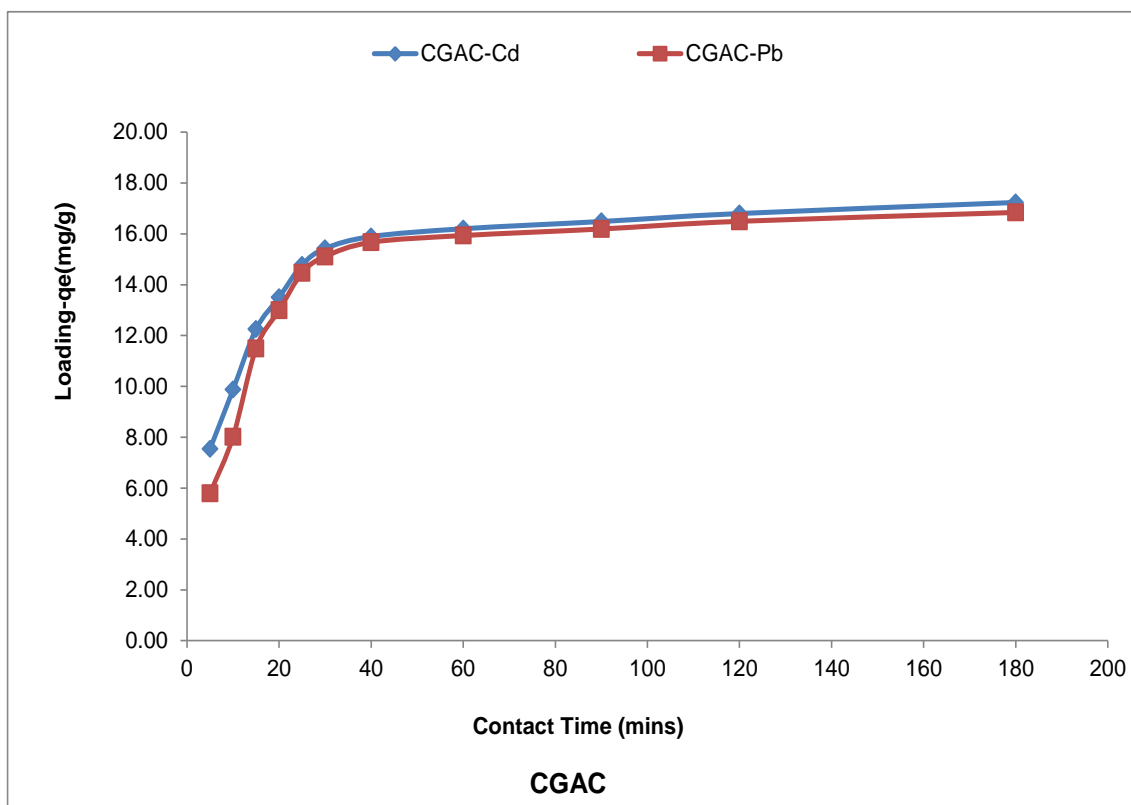


Figure 12: Effect of contact time on metal ion loading on CGAC adsorbent

The two stage kinetic profile for both Cd(II) and Pb(II) ions can be associated to the nature and types of available surface sites for adsorption. When the sorbent-sorbate contact is established at the onset of sorption there are a large number of available sites for sorption to occur, hence the fast metal ion uptake observed. However, as the uptake proceeds and readily available sites are occupied, the rate of further adsorption is diminished due a combination of factors such as repulsive forces between the already adsorbed metal ions and the incoming sorbate and the limitation of available sites for occupation. This gradual occupancy of the remaining available sites will thus proceed at a slower rate than when there were abundant sites at the inception of the sorption. This two-phase trend in sorption kinetics has been also reported in literature by a number of studies.

Ibrahim *et al.*, (2010) reported that the adsorption of Pb(II) ions onto a novel agricultural waste adsorbent (modified soda lignin) proceeded via a fast initial stage and a slow second stage until the attainment of equilibrium. A sharp increase in the amount of Cu(II) ion adsorbed by chemically modified orange peel within an initial duration of (0-30minutes) that was followed by a slow sorption until 120 minutes has also been reported by Feng *et al.*, (2009). Similar conclusions on the effect of contact time on sorption of adsorbate onto adsorbents have been proposed by studies reported in literature (El-Ashtoukhy *et al.*, 2008; Iqbal *et al.*, 2009b).

According to Liang *et al.*, (2010), this fast and slow two step kinetic sorption regime for the removal of metal ions has significant practical importance in the design of large scale adsorption systems and would imply that if a scale up system is to be designed. The adsorber has to be configured in such a manner that the fast kinetics profile observed for this type of adsorbent is exploited to improve removal efficiency within a short time interval. This may require a system that allows for optimum contact of the adsorbate system with the adsorbent with an efficient mixing cycle.

### 3.2.1 Kinetic modelling of Cd(II) and Pb(II) ion sorption on CGAC adsorbent

The uptake of Pb(II) and Cd(II) ions by the CGAC adsorbent was also modelled using two adsorption reaction models-the pseudo first order (PFO) and the pseudo second order (PSO) equations which have been discussed previously. The PFO and PSO models were evaluated using the non-linear method, a trial and error procedure. This method is designed to determine isotherm parameters by minimizing the respective coefficient of determination between experimental data and isotherm models using the solver add-in in Microsoft excel (Brown, 2001; Wong *et al.*, 2004). To determine the goodness of fit of the kinetic models to the experimental data using non-linear regression, the optimization procedure requires that error functions be defined to enable the fitting of the model parameters with the experimental values. In this study, the coefficient of determination ( $r^2$ ), the root mean square error (RMSE) and the Chi square test ( $\chi^2$ ) were used as error parameters for each model and these were determined based on eqns. 19-21.

#### *Pseudo first and second order kinetic modelling*

The plots of the PFO and PSO models for Cd(II) sorption by the CGAC adsorbents are presented in Fig. 13 for Cd(II) ion and 14 for Pb(II) ion. From these models, the kinetic parameters and their respective error functions obtained are presented in Table 2. An examination of Fig. 13 and 14 indicates that both PFO and PSO could be used to characterise the kinetics of metal ion sorption and their prediction of the parameter ( $q_{e,model}$ ) is close to the result obtained from the experimental analysis of Pb(II) and Cd(II) ion sorption. For the PFO model the  $q_{e,cal}$  obtained for the GCAC adsorbent for Cd(II) ion sorption was  $16.5 \text{ mgg}^{-1}$ , while that for Pb(II) was  $16.4 \text{ mgg}^{-1}$  indicating a close association of the sorption of both metal ions. The rate constant of the pseudo first order reaction ( $K_1$ ) for the two metal ions were;  $9.43 \times 10^{-2} \text{ min}^{-1}$ (CGAC-Cd) and  $7.77 \times 10^{-2} \text{ min}^{-1}$ (CGAC-Pb). The value of the coefficient of

determination ( $r^2$ ) and the two error parameters – the root mean square (RMSE) and Chi square ( $\chi^2$ ) can be used to determine the metal ion uptake kinetics is best described by the PFO model.

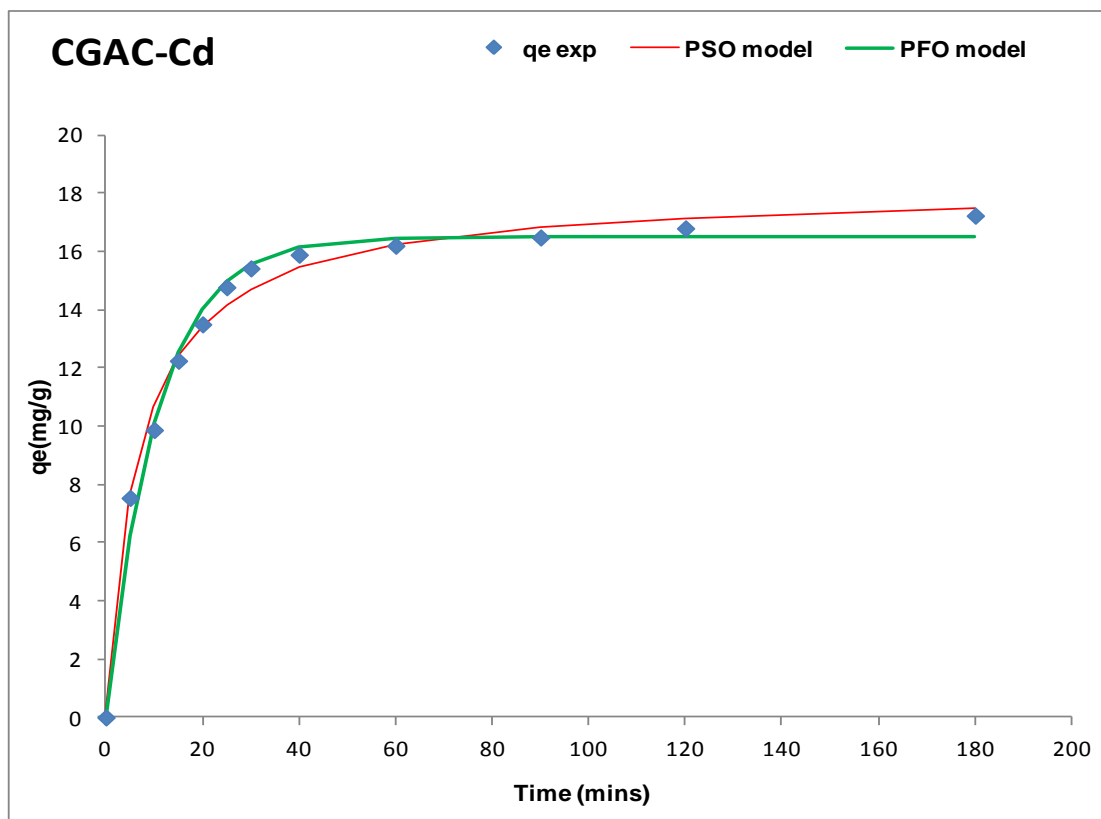


Figure 13: PFO & PSO kinetic models for Cd(II) ion sorption onto CGAC adsorbent

From Table 2, it is observed that both metal ions had the same  $r^2$  value of 0.99. Hence, to further discriminate amongst them, the  $\chi^2$  and the RMSE values are used with the lower values being an indication of a better fitting to the experimental data. Based on this assumption, the sorption of Pb(II) ion onto the CGAC adsorbent is best described by the PFO model with the lower  $\chi^2$  (0.01) and RMSE ( $7.10 \times 10^{-2}$ ) values.

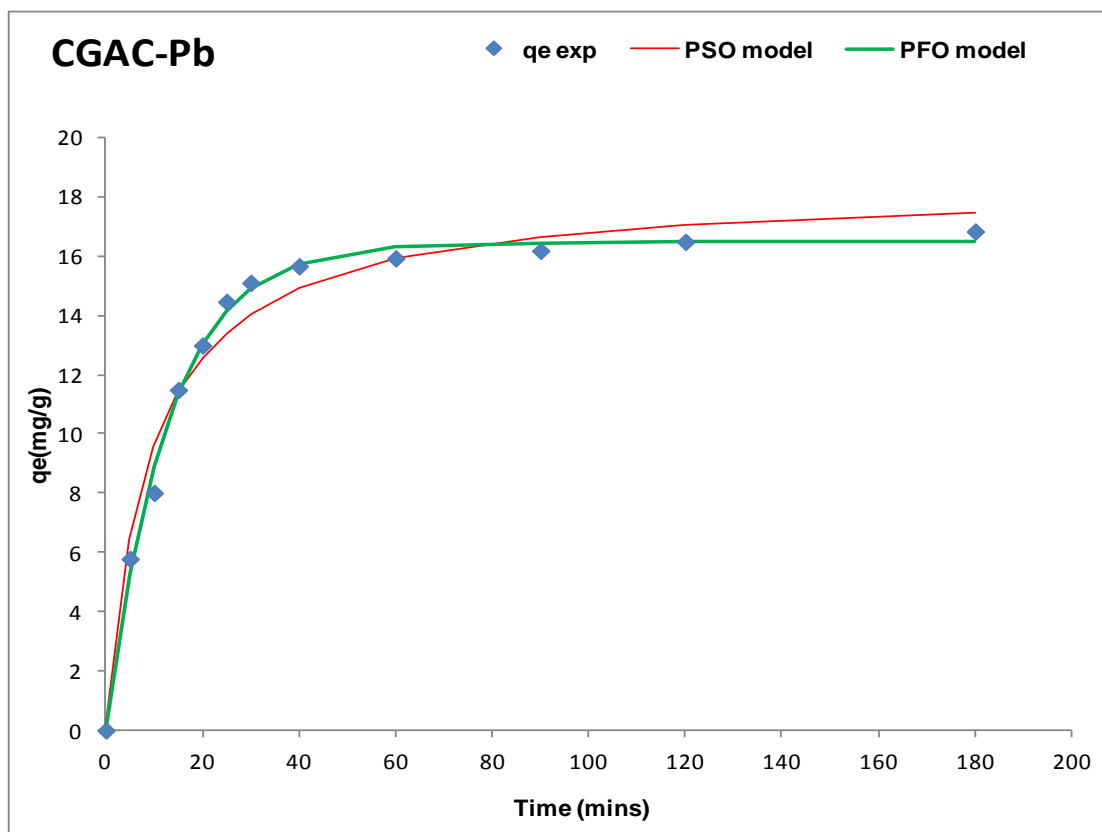


Figure 14: PFO & PSO kinetic models for Pb(II) ion sorption onto CGAC adsorbent

The PSO model evaluation of the kinetics of CGAC sorption of Pb(II) and Cd(II) ions are presented also presented in Table 2. From this table the PSO rate constant ( $K_2$ ) for Cd(II) ion was  $7.80 \times 10^{-3} \text{ gm}^{-1}\text{min}^{-1}(\text{CGAC-Cd})$  while that for Pb(II) was  $5.88 \times 10^{-3} \text{ gm}^{-1}\text{min}^{-1}(\text{CGAC-Pb})$ . From this model, the initial sorption rate ( $h$ ) obtained from the PSO model as  $q_t/t \rightarrow 0$  which gives an indication of the initial kinetic rate of sorption was  $2.59 \text{ mgg}^{-1}\text{min}^{-1} (\text{CGAC-Cd})$  and  $2.59 \text{ mgg}^{-1} \text{ min}^{-1} (\text{CGAC-Pb})$ . This indicates that the sorption of Cd(II) ions onto the CGAC adsorbent was faster than that of Pb(II) ions. The values of the metal ion loading obtained from the PSO model ( $q_{e,\text{cal}}$ ) was  $18.1 \text{ mgg}^{-1} (\text{CGAC-Cd})$  and  $18.4 \text{ mgg}^{-1}(\text{CGAC-Pb})$  indicating a higher loading of Pb(II) ions onto the commercial activated carbon adsorbent than Cd(II) ions.

Table 2: PFO and PSO kinetic parameters for Cd(II) &amp; Pb(II) sorption on CGAC

Kinetic Models	Parameters	Adsorbent	
		CGAC-Cd	CGAC-Pb
Pseudo First Order (PFO)	$q_{e,cal}(mgg^{-1})$	16.5	16.4
	$K_1(min^{-1})$	9.43E-02	7.77E-02
	$r^2$	0.99	0.99
	RMSE	1.32E-01	7.10E-02
	$\chi^2$	0.02	0.01
Pseudo Second Order(PSO)	$q_{e,cal}(mgg^{-1})$	18.1	18.4
	$K_2(gmg^{-1}min^{-1})$	7.88E-03	5.88E-03
	$h(mgg^{-1}min^{-1})$	2.59	1.99
	$r^2$	0.99	0.98
	RMSE	9.22E-02	3.05E-01
	$\chi^2$	0.01	0.04

The value of the coefficient of determination ( $r^2$ ) and the two error parameters – the root mean square (RMSE) and Chi square ( $\chi^2$ ) can be used to determine the kinetics of metal ion sorption that is best described by the PSO model. The value of the error parameters and the  $r^2$  value for both metals for the PSO model are presented in Table 2. From table 2 it is observed that the CGAC-Cd adsorbent had a higher  $r^2$  value (0.998) than the CGAC-Pb adsorbent. An evaluation of the two error parameters and the value of  $q_{e, cal}$  from the two models compared to the experimental value  $q_{e,exp}$  indicates that the CGAC adsorbent uptake of Cd(II) ion is better described by the PSO model with the lower  $\chi^2$  (0.01) and RMSE ( $9.822 \times 10^{-2}$ ) values, while the PFO model describes the sorption of Pb(II) ion better. This suggest that based on the kinetic modelling results, the rate limiting step of Pb(II) ion sorption onto the CGAC adsorbent is dependent on the concentration of the Pb(II) ions in the adsorbate, while the sorption of Cd(II) ions onto the CGAC adsorbent has a chemisorption rate-controlling mechanism (Kumar *et al.*, 2010). However, the closeness of the parameters obtained from the PSO and PFO models for the sorption of both ions (Cd(II) and Pb(II)) can be used to infer that chemical interactions between the ions in the adsorbate solution and the adsorbent may still influence sorption kinetics but this may depend on the rate of diffusion. This implies that pore diffusivity of the ions onto the active sites may also influence the kinetics as previously discussed in the analysis of the two stage

metal uptake (fast and slow) kinetics of Cd(II) and Pb(II) ions sorption. The results obtained in this study for the kinetics of Cd(II) and Pb(II) ions is similar to what has been reported by Yang *et al.*, (2014) on the kinetics of Pb(II) ion sorption using a commercial activated carbon adsorbent (AC). In their study, the kinetic modelling based on the PSO and PFO models were used to determine that the rate controlling mechanism for Pb(II) sorption onto the adsorbent was based on chemisorption.

#### *Intraparticle diffusion kinetic modelling*

The Weber and Morris intraparticle diffusion model was also used to describe the kinetics of Cd(II) and Pb(II) sorption. The assumption in the model is that if the regression of  $q_t$  vs  $t^{1/2}$  is linear and passes through the origin, the intra-particle diffusion is the sole rate limiting step (Huang *et al.*, 2014; Mittal *et al.*, 2007). However, this is not always the case as other processes such as surface diffusion and equilibrium adsorption may also be rate limiting for different stages of the kinetic profile and this will result in multi-linearity in the intraparticle diffusion plot (Fierro *et al.*, 2008; Basha *et al.*, 2009; Qiu *et al.*, 2009). The plot of the Weber and Morris intraparticle diffusion model for the adsorption of Cd(II) and Pb(II) ions onto the CGAC adsorbent is shown in Figures 15 and 16 and Table 3 presents the model parameters obtained from the plots.

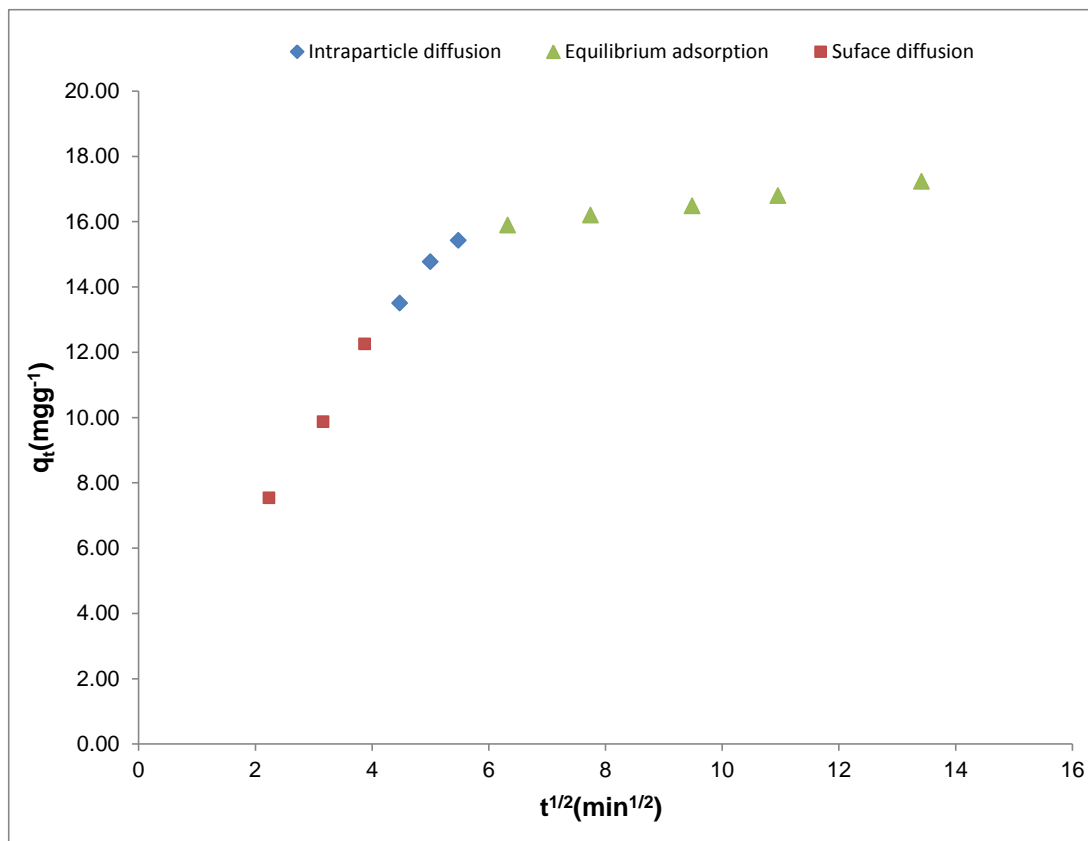


Figure 15: Kinetic stages in intraparticle diffusion plot of Cd(II) ion sorption on CGAC

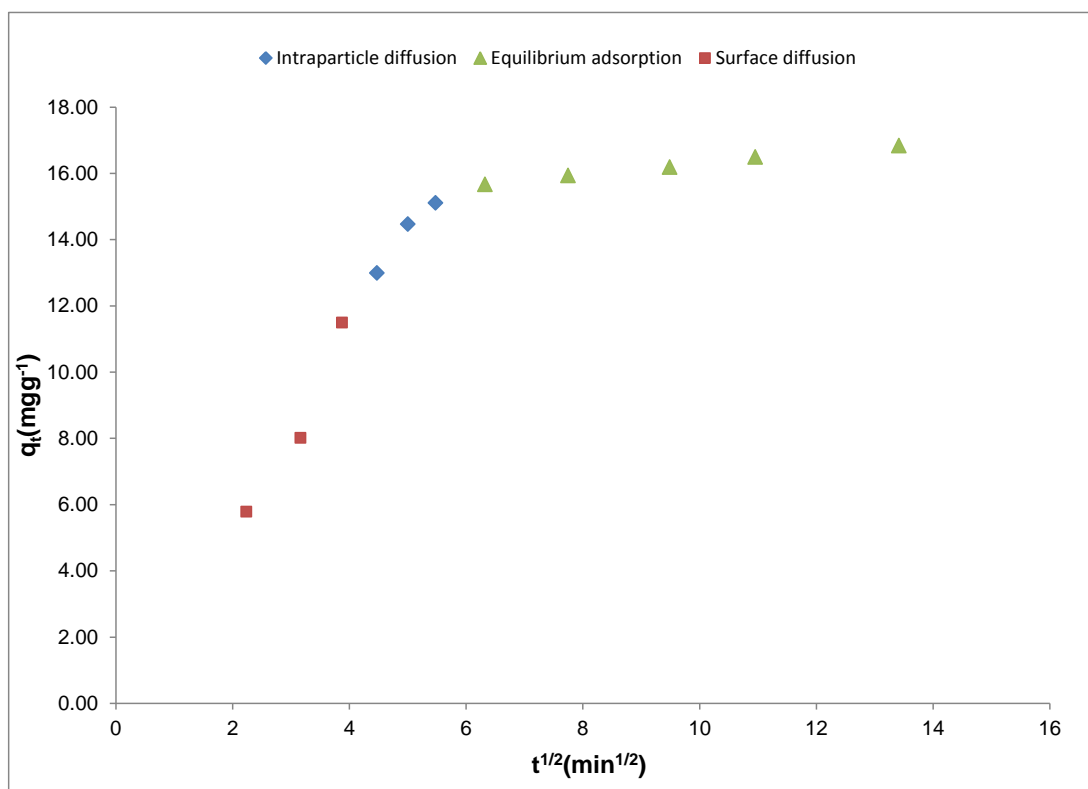


Figure 16: Kinetic stages in intraparticle diffusion plot of Pb(II) ion sorption on CGAC

Table 3: Intraparticle diffusion parameters for CGAC sorption of Cd(II) and Pb(II) ions

Kinetic Stages	Parameters	CGAC-Cd	CGAC-Pb
Surface diffusion stage	$K_{id}(\text{m}g\text{g}^{-1}\text{min}^{-0.5})$	2.86	3.43
	C	1.04	2.17
	$r^2$	0.99	0.96
Intraparticle diffusion stage	$K_{id}(\text{m}g\text{g}^{-1}\text{min}^{-0.5})$	1.92	2.11
	C	4.99	3.65
	$r^2$	0.98	0.96
Equilibrium adsorption stage	$K_{id}(\text{m}g\text{g}^{-1}\text{min}^{-0.5})$	0.19	0.17
	C	14.7	14.6
	$r^2$	0.99	0.99

From Fig.15 and 16 and Table 3, it is observed that multi-linear regions exist in the intraparticle diffusion plot which may indicate that the sorption of Cd(II) and Pb(II) ions onto the CGAC adsorbent occurred via 3 phases and these are:

- The first phase represents the region of external surface diffusion which is an instantaneous process due to the availability of sufficient adsorption sites on the CGAC adsorbent. Here, film diffusion may pre-dominate the kinetics of Cd(II) and Pb(II) uptake due to the diffusion of the ions across the boundary layer from the aqueous solution onto the adsorbent surface. In this region, the diffusion rate is highest for both ions,  $\{K_{id}= 2.86 \text{ m}g\text{g}^{-1}\text{min}^{-0.5}$  for Cd(II) and  $3.43 \text{ m}g\text{g}^{-1}\text{min}^{-0.5}$  for Pb(II) $\}$  due to the presence of sufficient surface area and adsorption sites (Huang *et al.*, 2014).
- The second phase describes a gradual sorption of the Cd(II) and Pb(II) ions onto the CGAC adsorbent pores from the mesopores to the micropores where it is suggested that the intraparticle diffusion of the metal ions within the pores of the adsorbent is rate limiting (Sengil *et al.*,2009). In this region, there exist on the adsorbent surface a layer due to the inter-ionic attraction and molecular association that exist between the adsorbate (ions) and the CGAC adsorbent active sites (Huang *et al.*, 2014). These thick layers may

results in a decrease in the rate of diffusion -{ $K_{id}= 1.92 \text{ mgg}^{-1}\text{min}^{-0.5}$  for Cd(II) and  $2.11 \text{ mgg}^{-1}\text{min}^{-0.5}$  for Pb(II)} in the adsorbent pores compared to the first stage for both ions.

- The final phase is the process associated with the attainment of equilibrium during the sorption process seen as the plateau region wherein the uptake is slowed due to the decreasing concentration of the ions in the adsorbate as well as the lower availability of active sites on the CGAC adsorbent for Cd(II) and Pb(II) ions uptake and the increasing repulsive interactions existing on the surface of the adsorbent (Basha *et al.*, 2009; Sengil *et al.*, 2009). The rate of diffusion in this region was the lowest amongst the three with -{ $K_{id}= 0.18 \text{ mgg}^{-1}\text{min}^{-0.5}$  for Cd(II) and  $0.16 \text{ mgg}^{-1}\text{min}^{-0.5}$  for Pb(II)} indicating the drive towards completion of the adsorption process.

From the intraparticle plot and the above observation, it should be noted that due to the existence of these multiple steps in the rate of ions uptake and since the intraparticle diffusion plot for the sorption both ions did not go through the origin, then the diffusion controlled sorption process can be said to have been controlled by the some other process described above and not just the intraparticle diffusion step. This also can be associated to the differences in the rate of mass transfer between the initial and final stages of adsorption. However, at each phase of the kinetic profile, it is assumed that only one mechanism was dominant (Fierro *et al.*, 2008; Diagboya *et al.*, 2014; Olu-Owolabi *et al.*, 2014). Furthermore, the value of the boundary layer parameter (C) obtained from the intraparticle diffusion plot for the removal of Cd(II) and Pb(II) ions by the CGAC adsorbent is presented in Table 3 for the different kinetic regimes and this gives an indication of the effect of the boundary layer thickness on the diffusion of both ions onto the activated carbon adsorbent. If the value of C is zero, this implies that the intraparticle diffusion mechanism is the only rate-limiting step of sorption, however, the higher, the value of C the greater the contribution of surface adsorption on the rate –limiting step of metal sorption.

Also, a higher value for C indicates that there is a greater effect of the boundary layer on metal ion diffusion across the adsorbent surface (Li *et al.*, 2012; Olu-Owolabi *et al.*, 2014). However, the multiple steps that are observed to operate based on the different kinetic models during the kinetics of Cd(II) and Pb(II) ions sorption suggest that there are a number of other factors that have to be taken into consideration in the evaluation of metal ion sorption in an aqueous system. These include the implications of the dilute aqueous system that adsorption is being carried out, the rate of change of adsorbate concentration with time as sorption progresses and the type of mass transport that might occur based on the nature of the adsorbent. All these parameters may in one way or the other influence the transport of the adsorbate ions through the concentration

barrier onto the adsorbent surface or active sites and have to be taken into consideration when evaluating the kinetics of sorption.

### 3.3 Equilibrium isotherm modelling

The knowledge of sorbate/sorbent interaction at equilibrium is an essential tool in adsorption design and the use of equilibrium isotherm is one of the common methods deployed to obtain this information. According to Yaneva *et al.*, (2013), the essential issue is the understanding of the specific relationship between the pollutant concentration and its uptake degree by the solid phase at constant temperature and this is used to construct adsorption isotherms. Equilibrium studies were carried out for the removal of Cadmium (II) and Lead (II) ions from aqueous system using the commercial activated carbon (CGAC). The range of initial metal ion concentration was from  $50 \text{ mgL}^{-1}$  to  $500 \text{ mgL}^{-1}$  as previously reported in experimental section of this work. The amount of CGAC used was 1 g and 0.2 L solution was used and the experiment was carried out at  $25^\circ\text{C}$  and a pH of 7.

From the study, metal ion loading on the adsorbent was calculated and in this study, the Langmuir and Freundlich isotherms were used to characterise the adsorption process. The Langmuir and Freundlich isotherm models were evaluated using the non-linear method, a trial and error procedure. This approach is designed to obtain isotherm parameters from the models by minimizing the respective coefficient of determination between experimental data and isotherm models using the solver add-in in Microsoft excel (Brown, 2001; Wong *et al.*, 2004). To determine the goodness of fit of the isotherm models to the experimental data using non-linear regression, the optimization procedure requires that error functions be defined to enable the fitting of the model parameters with the experimental values. In this study, the coefficient of determination ( $r^2$ ), the root mean square error (RMSE) and the Chi square test ( $\chi^2$ ) were used as error parameters for each model and these were determined based on eqns. 19-21. The isotherms obtained for the sorption of Cd(II) ions are shown in Fig. 17 and that for Pb(II) are presented in Fig.18. From the isotherm plots, the isotherm parameters were obtained and are presented in Table 4.

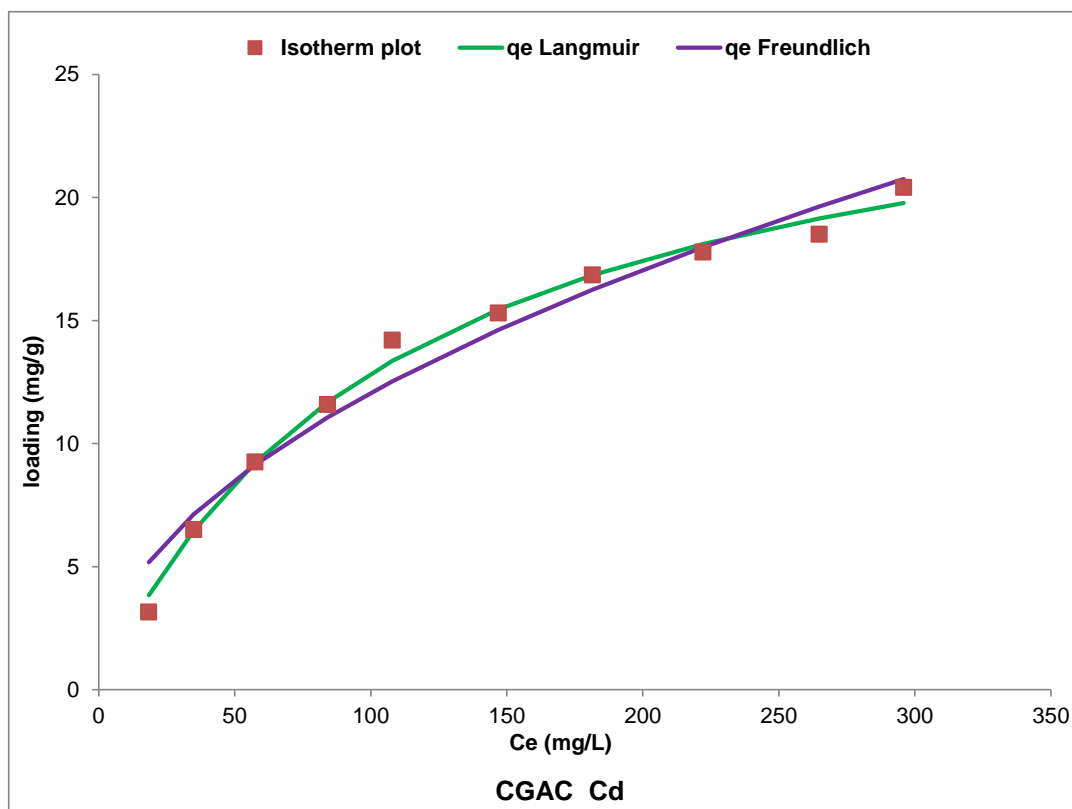


Figure 17: Langmuir & Freundlich adsorption isotherms for Cd (II) ions on CGAC

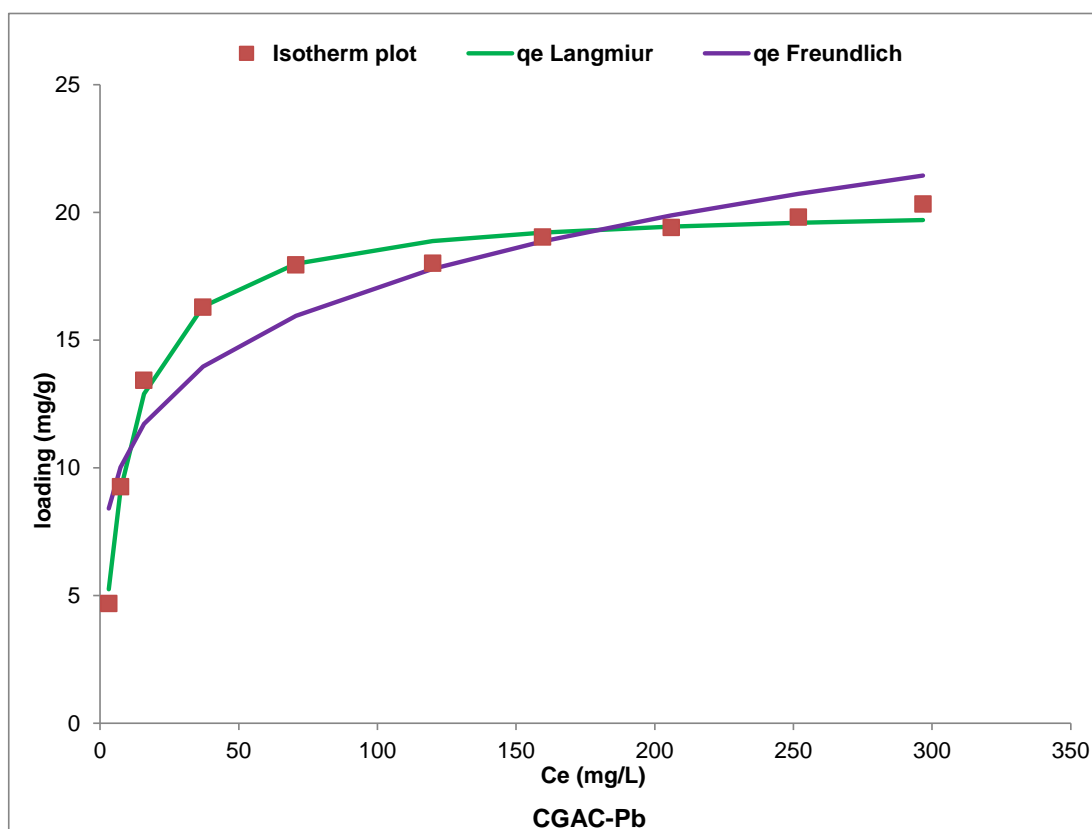


Figure 18: Langmuir & Freundlich adsorption isotherms for Pb (II) ions on CGAC

Table 4: Isotherm Parameters for Cd (II) and Pb (II) ions sorption on CGAC

Isotherm Models	Parameters	Adsorbent	
		CGAC-Cd	CGAC-Pb
Langmuir	$q_{\max}(\text{mgg}^{-1})$	27.3	20.3
	$K_L(\text{Lmg}^{-1})$	4.50E-02	1.10E-01
	$r^2$	0.95	0.99
	$\chi^2$	1.38E-01	1.10E-02
	RMSE	1.55	0.11
Freundlich	$K_F(\text{mgg}^{-1})(\text{Lmg}^{-1})^{1/n}$	6.99	6.63
	n	4.00	4.85
	$r^2$	0.86	0.87
	$\chi^2$	3.21E-01	1.83E-01
	RMSE	3.90	1.86

For Cd(II) ion sorption, an examination of Fig. 17 indicates that the metal ion loading on the adsorbent increased from  $3.15 \text{ mgg}^{-1}$  for an initial metal ion concentration of  $50 \text{ mgL}^{-1}$  to  $20.41 \text{ mgg}^{-1}$  for  $500 \text{ mgL}^{-1}$  and from Fig. 18 it can be observed that the loading of Pb(II) on the CGAC adsorbent increased with increase in initial metal ion concentration from  $4.68 \text{ mgg}^{-1}$  for  $50 \text{ mgL}^{-1}$  to  $20.32 \text{ mgg}^{-1}$  for  $500 \text{ mgL}^{-1}$  of adsorbate. These equilibrium data were then fed into the Excel solver add-in program to provide an optimisation process for obtaining the isotherm parameters and the results from the process are shown in Table 4. The Freundlich isotherm is based on the assumption of an exponential distribution of adsorption sites and energies-heterogeneous surface (Hashemian *et al.*, 2013). The Freundlich constant “ $K_F$ ” which relates to adsorption capacity for both metal ion loading on CGAC adsorbent were  $1.20 (\text{mgg}^{-1})(\text{Lmg}^{-1})^{1/n}$  for Cd(II) and  $6.63 (\text{mgg}^{-1})(\text{Lmg}^{-1})^{1/n}$  for Pb(II). This indicates that based on the Freundlich adsorption assumption model, the loading of Pb(II) was higher than that of Cd(II) on the CGAC adsorbent. Furthermore, the Freundlich constant “n” which relates to the intensity of adsorption (Hashemian *et al.*, 2013) were 1.99 for Cd(II) and 4.85 for Pb(II) indicating more favourability of the Pb(II) ion sorption on the CGAC adsorbent.

The Langmuir isotherm assumes that the surface has homogeneous binding sites, equivalent sorption energies and no interaction between adsorbed species and its relevant parameters are Langmuir constant “ $K_L$ ” which refers to the energy constant related to the heat of adsorption capacity and “ $q_{max}$ ” which represents the maximum loading capacity of the adsorbent (Hashemian *et al.*, 2014). For the two metal ions the Langmuir constant value was  $8.8 \times 10^{-3}$   $Lmg^{-1}$  for Cd(II) and  $1.10 \times 10^{-1}$   $Lmg^{-1}$  for Pb(II) indicating that the Pb(II) loading onto the surface of the CGAC has a lower heat of adsorption. The Langmuir loading capacity constant for Cd(II) was  $27.29$   $mgg^{-1}$  and that of Pb(II) was  $20.30$   $mgg^{-1}$ . This indicates the value for the maximum amount of metal ion that can adsorbed on the CGAC adsorbent, thereby implying that the loading of Cd(II) was higher on the adsorbent than that of Pb(II) ion.

A comparison of the fitting of the two models to the experimental data was also carried out based on the parameters obtained from the two models. The fitting parameters were the coefficient of determination- $r^2$ , the two error parameters- chi square ( $\chi^2$ ) and root mean square error (RMSE) and these are presented in Table 4. From Table 4, it can be observed that the Langmuir model describes the uptake of Pb(II) ion by the CGAC adsorbent better than that of the Cd(II) ion as its  $r^2$  value is higher for Pb(II) ion than Cd(II) ion, while the values of RMSE and  $\chi^2$  are lower for Pb(II) ion than Cd(II) ion. For the Freundlich model, the same observation can also be made as the isotherm fits the Pb(II) ion better than that of the Cd(II) ion based on the values of  $r^2$ ,  $\chi^2$  and RMSE. Comparison of the isotherm model parameters for the two isotherms indicates that the Langmuir isotherm fits the experimental sorption data better than the Freundlich model as its  $r^2$  values for both Cd(II) and Pb(II) ions sorption are higher than those for the respective ions for the Freundlich. In addition the values for the two error parameters- RMSE and  $\chi^2$  are significantly lower for the Langmuir model than for the Freundlich. Hence the Langmuir isotherm is the better isotherm for the description of Cd(II) and Pb(II) ions sorption by the CGAC adsorbent.

Previous studies on the adsorption of Cd(II) ion commercial activated carbon (CAC) has been reported by Kannan and Rengasamy (2005) and the Langmuir loading capacity obtained from the study was  $4.29$   $mgg^{-1}$  and a Langmuir constant “ $K_L$ ” value of  $9.84$   $Lmg^{-1}$ . In a similar work, Goel *et al.*, (2005) reports on the removal of Pb(II) using granular activated carbon via batch and column sorption and their Langmuir constant “ $K_L$ ” was  $3.5$   $Lmg^{-1}$  and the Langmuir maximum loading constant “ $q_{max}$ ” was  $21.88$   $mgg^{-1}$ . They also reported Freundlich isotherm constant values of  $11.49$  ( $mgg^{-1})(Lmg^{-1})^{1/n}$  for “ $K_F$ ” and  $2.44$  for the “ $n$ ” Freundlich constant.

A comparison of the values of the Langmuir isotherm parameter  $q_{\max}$  obtained in this study with those reported in previous studies for the sorption of Cd(II) and Pb(II) ions from aqueous solutions using commercial activated carbon adsorbents was also carried out and are presented in Tables 5 and 6.

Table 5: Comparison of Langmuir constant ( $q_{\max}$ ) with reported literature for Cd(II) ion

Adsorbent	$q_{\max}$ (mgg <sup>-1</sup> )	Reference
Commercial activated carbon (AC)	10.3	Hydari <i>et al.</i> , 2012
Commercial activated carbon pellets	16.2	Bian <i>et al.</i> , 2015
Commercial activated carbon (CAC)	4.29	Kannan and Rengasamy, 2005
Granular commercial activated carbon (GAC)	11.7	Wasewar <i>et al.</i> , 2010
Granular activated carbon (GAC)	10.1	Moreno-Castilla <i>et al.</i> , 2004
Activated carbon	6.75	Sanchez- Polo and Rivera-Utrilla, 2002
Commercial activated carbon (CA)	9.77	Correa <i>et al.</i> , 2012
Commercial activated carbon (CGAC)	27.3	This study

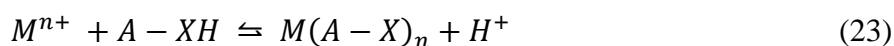
Table 6: Comparison of Langmuir constant ( $q_{\max}$ ) with reported literature for Pb(II) ion

Adsorbent	$q_{\max}$ (mgg <sup>-1</sup> )	Reference
Commercial activated carbon (AC)	21.8	Goel <i>et al.</i> , 2005
Commercial activated carbon	47.2	Largitte <i>et al.</i> , 2014
Commercial granular activated carbon	43.1	Largitte and Laminie , 2015
Commercial granular activated carbon (GAC)	10.8	Machida <i>et al.</i> , 2005
Commercial activated carbon (CAC)	5.95	Kannan and Veemaraj, 2009
Commercial activated carbon (CGAC)	20.3	This study

From both Tables 5 & 6, it can be observed that the maximum loading obtained using the CGAC adsorbent for the sorption of Cd(II) and Pb(II) ions are within the range of what has been reported previously in literature for some commercial activated carbon adsorbents. Thus, it can be inferred that CGAC used in this study was a good adsorbent for Cd(II) and Pb(II) ions removal from aqueous systems as its characteristics and loading parameters are within the range of some reported studies in literature for commercial activated carbon adsorbents.

### 3.4 Mechanism of Cd(II) and Pb(II) ion sorption on CGAC adsorbent

The degree of interaction of the Cd(II) and Pb(II) ion species with the other ionic species in the adsorbate system is presumed to affect the amount of the target ions that are preferentially adsorbed onto the surface of the CGAC adsorbent. This interaction can be used to explain the variation in the loading of the two ions onto the CGAC adsorbent surface. The sorption studies reported for these two ions was carried out at pH 7.0 based on the zeta potential analysis of the CGAC adsorbent which has been previously discussed. Thus, the adsorption of the two metal ions in the adsorbate at this pH may be due to the interaction of the species that are dominant at  $\text{pH} < 8$ , such as  $\text{Pb}^{2+}$ ,  $\text{Cd}^{2+}$ ,  $\text{Pb}(\text{OH})^+$  and  $\text{Cd}(\text{OH})^+$  with the functional groups on the adsorbent surface (Kikuchi *et al.*, 2006). These species of the two metal ions that can interact with the functional groups on the adsorbent improves the probability of metal ion removal. Thus due to the multiple-ion-binding sites on the adsorbent surfaces and the variety of metal ion species in the adsorbate a number of metal adsorbent complexes are formed during sorption process. This can be represented according to eqn.22 (Akpomie *et al.*, 2015; Rao *et al.*, 2010; Hu *et al.*, 2015):



Where M= metal; A-XH (Adsorbent surface); [X=S, O, COO, NH];  $M(A-X)_n$  –metal adsorbent complex and  $H^+$  - Displaced proton.

Hence, based on the results obtained from the EDX analysis, the sorption of Cd(II) and Pb(II) ions by the CGAC adsorbent may take place by ion exchange where the metal ion displaces the proton ( $H^+$ ) from the adsorption site and becomes attached to the adsorbent forming an adsorbent metal complex. Therefore, speciation plays a significant role in the determination of the amount of metal adsorbed, especially when consideration is given to the ionic radii and ionic charge of the metal. According to Atkinson *et al.*, (1998), the assumption in an adsorbate system is that when there is electrical attraction between adsorbates, ions with small ionic radii but higher ionic charge are more strongly attracted to sites of opposite charge (adsorbent). However, for ions of similar charge, the hydrated radius of the hydrated metal ions determines the order of preference and for sorption, metals with ions of smaller ionic radii move closer to potential adsorption sites (Atkinson *et al.*, 1998). This mechanism can be used to explain the higher uptake capacity for Cd(II) ion when compared with Pb(II) ions by the CGAC adsorbent

investigated in this study. The variation in  $q_{\max}(\text{mgg}^{-1})$  and  $q_e(\text{mgg}^{-1})$  for the respective adsorbents may be attributed to the differences in the ionic sizes of Cd(II) and Pb(II) ions. The ionic radius of Cd(II) is  $0.97\text{\AA}$ , while that of Pb(II) is  $1.20\text{\AA}$ . Hence due to the smaller ionic size of Cd(II) ion, in the adsorbate system it will exhibit greater affinity to the active sites on the different adsorbents due to its smaller hydrated radius which would aid faster diffusion from the adsorbate system onto the adsorbent surface. This trend has also been reported by Horsfall *et al.*, (2006) in their study on the sorption of Cd(II), Cu(II) and Zn(II) ions from aqueous solutions by cassava (*Manihot sculenta* Cranz) tuber bark waste.

#### 4. Conclusions

The characterisation and use of a commercial activated carbon (CGAC) for Cd(II) and Pb(II) metal ion sorption studies was carried out in this study. The activated carbon had high surface area and porosity properties and SEM and EDX analysis of the fresh and used adsorbents gave insight into the morphology and chemical nature of the adsorbents. The CGAC adsorbent had a high BET surface area of  $4273\text{m}^2\text{g}^{-1}$ , with a total pore volume of  $2.66\text{ cm}^3\text{g}^{-1}$  and it had pores with average diameter of  $4.48\text{nm}$ . Thus the CGAC adsorbent can be considered to be a mesoporous activated carbon adsorbent with high surface area and considerable pore volume. The adsorbent morphology showed that the adsorbent surface was rough and coarse with irregular crevices. The results of the EDX analysis of the CGAC adsorbent before and after Cd(II) and Pb(II) ion sorption indicated the presence of the two ions on the adsorbent surface and confirmed the observation that the CGAC adsorbent was able to remove these metal ions from their respective aqueous systems. Thermogravimetric analysis of the CGAC adsorbent indicated a total weight loss under thermal decomposition of 7.6%, which implies that the adsorbent was made up about 90% carbon that was stable under the thermal degradation conditions. FTIR characterisation indicated the presence of carboxyl, amides, ethers, and cyano and nitro groups which are presumed as the active sites on the CGAC adsorbent for the uptake of Cd (II) and Pb (II) ions from the aqueous adsorbate system.

Kinetic and equilibrium metal ion sorption studies were carried out and the adsorbent showed a considerable loading of the two metal ions. The kinetics of Cd(II) and Pb(II) ions sorption using the CGAC adsorbent showed a two-stage kinetic profile- initial quick uptake occurring within 30 minutes followed by a slow and gradual removal of the two metal ions until 180 minutes. The kinetics also indicated that optimum loading obtained after 180 minutes of experiment was  $17.23\text{ mgg}^{-1}$  and  $16.84\text{ mgg}^{-1}$  for Cd(II) and Pb(II) ions respectively. The kinetic modelling

using the pseudo first order (PFO) and pseudo second order (PSO) models indicates that the PFO model described the sorption of Pb(II) ion better, while the PSO described the sorption of Cd(II) ion better. Intraparticle diffusion kinetic modelling indicated that intraparticle diffusion may not be the only mechanism that influenced the rate of ions uptake onto the CGAC adsorbent due to the presence of multi-linear stages in the profile.

Isotherm modelling was carried out using Langmuir and Freundlich models and it was observed that the Langmuir and Freundlich models describes the uptake of Pb(II) ion by the CGAC adsorbent better than that of the Cd(II) ion. A comparison of between the two models indicates that the Langmuir isotherm is the better isotherm for the description of Cd(II) and Pb(II) ions sorption by the CGAC adsorbent. The maximum loading capacity ( $q_{\max}$ ) obtained from the Langmuir isotherm was  $27.3\text{mgg}^{-1}$  and  $20.3\text{mgg}^{-1}$  for Cd(II) and Pb(II) ions respectively, thus indicating that CGAC adsorbent had higher affinity for the Cd(II) ion. These metal ion uptake values obtained for the CGAC adsorbent were comparable to those reported in previous literature for Cd(II) and Pb(II) removal using activated carbon adsorbents indicating that this adsorbent can be an effective material for the removal of metal ions from aqueous systems, effluents and wastewater.

## References

- Acharya, J.; Sahu, J. N.; Mohanty, C. R. and Meikap, B. C. (2009) Removal of lead(II) from wastewater by activated carbon developed from Tamarind wood by zinc chloride activation. *Chemical Engineering Journal*, 149: 249-262.
- Adekunle, A.S.; Oyekule, J.A.O.; Baruwa, S.O; Ogunfowokan, O.A. and Ebenso, E.E.(2014) Speciation study of the heavy metals in commercially available recharge cards coatings in Nigeria and the health implications. *Toxicology Reports*, 1: 243-251
- Agudelo-Castaneda, D.; Teixeira, E. C.; Schneider, I. L. and Rolim, S. B. A.; Balzaretti, N. and Silva, G. S. (2015) Comparison of emissivity, transmittance, reflectance infrared spectra of polycyclic aromatic hydrocarbons with those of atmospheric particulates (PM<sub>1</sub>). *Aerosol and Air Quality Research*, 15: 1627-1639.
- Ahmadi, K.; Ghaedi, M. and Ansari,A.(2015) Comparison of nickel doped zinc sulphide and/or palladium nanoparticle loaded on activated carbon as efficient adsorbents for kinetic and equilibrium study of removal of Congo Red dye. *Spectrochimica Acta Part A: Molecular and Biomolecular Spectroscopy*, 136:1441-1449.
- Ahmedna, M.; Marshall, W.E. and Rao, R.M.(2000) Production of granular activated carbons from select agricultural by-products and evaluation of their physical, chemical and adsorption properties, *Bioresource Technology*,71(2):113-123.
- Akpomie, K.G.; Dawodu, F.A. and Kayode O. Adebowale, K.O. (2015) Mechanism on the sorption of heavy metals from binary-solution by a low cost montmorillonite and its desorption potential. *Alexandria Engineering Journal*, 54(3): 757-767.
- Ali, R. M.; Hamad, A. A.; Hussein, M. M. and Malash, G. F. (2016) Potential of using green adsorbent of heavy metal removal from aqueous solutions: Adsorption kinetics, isotherm, thermodynamics, mechanisms and economic analysis. *Ecological Engineering*, 91:317-332.
- Alkan, M.; Demirbaş, Ö. and Doğan, M., (2007) Adsorption kinetics and thermodynamics of an anionic dye onto sepiolite. *Microporous and Mesoporous Materials*, 101(3):388-396.
- Alkan, M.; Karadas, M.; Dogan, M. and Demirbas, O. (2009) Zeta potentials of perlites samples in various electrolyte and surface media. *Colloids and Surfaces A: Physicochemical and Engineering Aspects*, 259(1-3):155-166.
- Al-Lagtah, N.M.A.; Al-Muhtaseb, A.H.; Ahmad, M.N.M and Salameh, Y. (2016) Chemical and physical characteristics of optimal synthesised activated carbons from grass-derived sulfonated lignin versus commercial activated carbons. *Microporous and Mesoporous Materials*, 225: 504-514.
- Anisuzzaman, S.M.; Joseph, C.G.; Taufiq-Yap, Y.H.; Krishnaiah, D. and Tay, V.V. (2015) Modification of commercial activated carbon for the removal of 2,4-dichlorophenol from simulated wastewater. *Journal of King Saud University-Science*, 27(4):318-330.
- Arena, N.; Jacquetta Lee, J. and Clift, R. (2016) Life Cycle Assessment of activated carbon production from coconut shells, *Journal of Cleaner Production*,125:68-77.

Asuquo, E.D and Martin, A.D. (2016) Sorption of cadmium (II) ion from aqueous solution onto sweet potato (*Ipomoea batatas* L.) peel adsorbent: Characterisation, kinetic and isotherm studies, *Journal of Environmental Chemical Engineering*, 4 (4) Part A: 4207-4228.

Athar, M.; Farooq, V.; Aslam, M. and Salam, M. (2013) Adsorption of Pb(II) ions onto biomass from *Trifolium resupinatum*: equilibrium and kinetic studies. *Applied Water Science*, 3:665-672.

Atkinson, B.W.; Bux, F and Kasan, H.C.(1998) Considerations for application of biosorption technology to remediate metal-contaminated industrial effluents. *Water SA*, 24(2)129-136.

ATSDR (2007) Agency for toxic substances and disease registry-Toxicological profile of lead. Available internet: <http://www.atsdr.cdc.gov/toxprofiles/tp13.pdf> Accessed on 12/01/2016.

ATSDR (2010) Agency for Toxic Substances and Disease Registry-Case Studies in Environmental Medicine (CSEM) Lead Toxicity. Available Internet: <http://www.atsdr.cdc.gov/csem/lead/docs/lead.pdf> Accessed on 20/12/2015

ATSDR (2012) Agency for toxic substances and disease registry-Public health statement on cadmium CAS # 7440-43-9 September, 2012. Available internet: <http://www.atsdr.cdc.gov/ToxProfiles/tp5-c1-b.pdf> Accessed on 12/12/2015.

Azarudeen, R.S.; Ahmed, M.A.R.; Subha, R. and Burkanudeen, A.R. (2015) Heavy and toxic metal ion removal by a novel polymeric ion-exchanger: Synthesis, characterisation, kinetics and equilibrium. *Journal of Chemical Technology Biotechnology*, 90:2170-2179.

Bacsik, Z.; Ahlsten, N.; Ziadi, A.; Zhao, G.; Garcia-Bennet, A.E.; Martin-Matute, B. and Hedin, N.(2011) Mechanism and kinetics for sorption of CO<sub>2</sub> on biocontinuous mesoporous silica modified with n-propylamine. *Langmuir*, 27:11118-11128.

Bailey, S. E.; Olin, T. J.; Bricka, M. R.; Adrian, D. D. (1999) A review of potentially low-cost sorbents for heavy metals. *Water Research*, 33(11): 2469-2479.

Basha, S.; Murthy, Z.V.P and Jha, B. (2009) Sorption of Hg(II) onto *Carica papaya*; Experimental studies and design of batch sorber. *Chemical Engineering Journal*, 147:226-234.

Bhattacharjee, S.; Chakrabarty, S.; Maity, S.; Kar, S.; Thakur, P. and Bhattacharyya, G. (2003) Removal of lead from contaminated water bodies using sea nodule as an adsorbent, *Water Research*, 37(16): 3954-3966.

Bian, Y.; Bian, Z.; Zhang, J.; Ding, A.; Liu, S.; Zheng, L. and Wang, H. (2015) Adsorption of cadmium ions from aqueous solutions by activated carbon with oxygen-containing functional groups. *Chinese Journal of Chemical Engineering*, 23(10):1705-1711.

Boag, N.M.; Haghgooeie, H. and Hassanzadeh, A. (2008) Synthesis and dynamic NMR studies of Pt( $\eta^5$ -C<sub>5</sub>Me<sub>5</sub>)(CO){C(O)NR<sub>2</sub>} complexes. *Spectrochimica Acta Part A: Molecular and Biomolecular Spectroscopy*, 69 (1): 156-159.

Brown, A. M. (2001) A step-by-step guide to non-linear regression analysis of experimental data using a Microsoft Excel Spreadsheet. *Computer Methods and Programs in Biomedicine*, 65: 191-200.

Cassol, G.O.; Gallo, R.; Schwaab, M.; Barbosa-Coutinho, E. ; Severo Jnr, J.B. and Pinto, J.C. (2014) Statistical evaluation of non-linear parameter estimation procedures for adsorption equilibrium models, *Adsorption Science and Technology*, 32(4):257-273.

Chand, P.; Shil, A.K.; Sharma, M. and Pakade, Y.B. (2014) Improved adsorption of cadmium ions from aqueous solution using chemically modified apple pomace: mechanism, kinetics and thermodynamics. *International Biodeterioration & Biodegradation*, 90:8-16.

Coleman N. T., McClung A. C. and Moore D. P. (1956) Formation constants for Cu(II)-peat complexes. *Science*, 123, 330-331.

Correa, M.L.; Velasquez, J.A. and Quintana, G.C. (2012) Uncommon Crop Residues as Ni(II) and Cd(II) Biosorbents. *Industrial & Engineering Chemistry Research*, 51;2456-12462.

Deng, S.; Wang, P.; Zhang, G.; Dou, Y. (2016) Polyacrylonitrile-based fiber modified with thiosemicarbazide by microwave irradiation and its adsorption behavior for Cd(II) and Pb(II), *Journal of Hazardous Materials*, 307: 64-72.

Diagboya, P. N; Olu-Owolabi, B. I. and Adebowale, K.O.(2014) Microscale scavenging of pentachlorophenol in water using amine and tripolyphosphate-grafted SBA-15 silica: Batch and modeling studies, *Journal of Environmental Management*, 146:42-49.

Dias, J. M.; Alvim-Ferraz, M.C.M.; Almeida, M.F.; Rivera-Utrilla, J.; Sánchez-Polo, M. (2007) Waste materials for activated carbon preparation and its use in aqueous-phase treatment: A review, *Journal of Environmental Management*, 85(4):833-846.

Dzul Erosa, M.S; Saucedo Medina, T. I.; Navarro Mendoza, R.; Avila Rodriguez, M. and Guibal, E. (2001) Cadmium sorption on chitosan sorbents: kinetic and equilibrium studies, *Hydrometallurgy*, 61(3):157-167.

El-Ashtoukhy, E.-S. Z.; Amin, N. K. and Abdelwahab, O. (2008) Removal of lead (II) and copper (II) from aqueous solution using pomegranate peel as a new adsorbent. *Desalination*, 223(2008): 162-173.

El-Khaiary, M.I. (2008) Least-squares regression of adsorption equilibrium data: comparing options. *Journal of Hazardous Materials*, 158(1):73-87.

El-Khaiary, M.I.; Malash, G.F. and Ho, Y.S. (2010) On the use of linearized pseudo-second-order kinetic equations for modeling adsorption systems, *Desalination*, 257(1-3):93-101

El-Shafey, E.I.; Ali, S.N.F.; Al-Busafi, S. and Al-Lawati, H.A.J. (2016) Preparation and characterisation of surface functionalized activated carbons from date palm leaflets and application for methylene blue removal, *Journal of Environmental Chemical Engineering*, 4(3):2713-2724.

Erdem, M.; Ucar, S.; Karagoz, S. and Turgay, T. (2013) Removal of Lead(II) ions from aqueous solutions onto activated carbon derived from waste biomass. *The Scientific World Journal*, article ID 146092, 7 pages. <http://dx.doi.org/10.1155/2013/146092>.

Farooq, U.; Khan, M.A; Athar, M. and Kozinski, J.A.(2011)Effect of modification of environmentally friendly adsorbent wheat (*Triticum aestivum*) on the biosorption removal of cadmium(II) ions from aqueous solution. *Chemical Engineering Journal*, 171:400-410.

Feng, N.; Guo, X. and Liang, S. (2009) Adsorption study of copper (II) by chemically modified orange peel. *Journal of Hazardous Materials* 164: 1286-1292.

Fernandez, M. E.; Ledesma, B.; Roman, S.; Bonelli, P. R. and Cukierman, A. L. (2015) Development and characterisation of activated hydrochars from orange peels as adsorbents for emerging organic contaminants. *Bioresource Technology*, 183: 221-228.

Fierro, V.; Torné-Fernández, V.; Montané, D.; Celzard, A.(2008) Adsorption of phenol onto activated carbons having different textural and surface properties, *Microporous and Mesoporous Materials*,111(1-3): 276-284.

Freundlich, H. M. F. (1906) Over the Adsorption in Solution. *Journal of Physical Chemistry*, 57: 385-471.

Ge, X.; Wu, Z.; Wu, Z.; Yan, Y.; Cravotto, G. and Ye, B. (2016) Microwave-assisted modification of activated carbon with ammonia for efficient pyrene adsorption. *Journal of Industrial and Engineering Chemistry*. <http://dx.doi.org/10.1016/j.jiec.2016.05.003>.

Gerçel, Ö. and Gerçel, F. H. (2007)Adsorption of lead(II) ions from aqueous solutions by activated carbon prepared from biomass plant material of *Euphorbia rigida*, *Chemical Engineering Journal*,132(1-3):289-297.

Goel, J.; Kadirvelu, K.; Rajagopal, C. and Garg, V. K. (2005) Removal of lead (II) by adsorption using untreated granular activated carbon: batch and column studies. *Journal of Hazardous Materials*, 125(1-3): 211-20.

Gimbert, F.; Morin-Crini, N.; Renault, F.; Badot, P. and Crini, G.(2008) Adsorption isotherm models for dye removal by cationized starch-based material in a single component system: Error analysis, *Journal of Hazardous Materials*,157(1)34-46

Greenwood, N. N. and Earnshaw, A. (2006) *Chemistry of the Elements*. 2<sup>nd</sup> Ed, Elsevier Ltd, Oxford.

Gupta, V.K.; Ganjali, M.R.; Nayak, A.; Bhushan, B. and Agarwal, S.(2012) Enhanced heavy metals removal and recovery by mesoporous adsorbent prepared from waste rubber. *Chemical Engineering Journal*, 197:330-342.

Gurses A., Hassani A., Kıransan M., Acıslı O. and Karaca S. (2014) Removal of methylene blue from aqueous solution using by untreated lignite as potential low-cost adsorbent: Kinetic, thermodynamic and equilibrium approach, *Journal of Water Process Engineering*, 2 10–21.

Hamad, H.; Ezzeddine, Z.; Lakis, F.; Rammal, H.; Srour, M.; Hijazi, A. (2016) An insight into the removal of Cu (II) and Pb (II) by aminopropyl-modified mesoporous carbon CMK-3: Adsorption capacity and mechanism, *Materials Chemistry and Physics*, 178:57-64

Harsh, H and Rodriguez-Reinoso, F. (2006) *Activated Carbon*, Elsevier Science &Technology Books, Elsevier Ltd, Oxford.

Hashemian, S.; Salari, K.; Hamila S. and Zahra A. Y. (2013) Removal of Azo Dyes (Violet B and Violet 5R) from Aqueous Solution Using New Activated Carbon Developed from Orange Peel. *Journal of Chemistry*, 2013: 1-10.

Hashemian, S.; Salari, K. and Yazdi, Z. A. (2014) Preparation of activated carbon from agricultural wastes (almond shell and orange peel) for adsorption of 2-pic from aqueous solution. *Journal of Industrial and Engineering Chemistry*, 20: 1892-1900.

Ho, Y.S. (2004a) Citation review of Lagergren kinetic rate equation on adsorption reactions. *Scientometrics*, 59(1):171-177.

Ho, Y.S. (2004b) Selection of optimum sorption isotherm. *Carbon*, 42 (2004) 2115–2116.

Ho, Y. S. (2006) Review of second-order models for adsorption systems. *Journal of Hazardous Materials, B* 136: 681-689.

Ho, Y. S. and Chiang, C. C. (2001) Sorption studies of acid dye by mixed sorbents. *Adsorption*, 7: 139-147.

Ho, Y. S. and McKay, G. (2000) The Kinetics of sorption of divalent metal ions onto sphagnum moss peat. *Water Research*, 34: 735-742.

Ho, Y. S.; Chiu, W. T.; Hsu, C. S.; Huang, C. T. (2004) Sorption of lead ions from aqueous solution using tree fern as a sorbent. *Hydrometallurgy*, 73: 55-61.

Ho, Y. S. and Ofomaja, A. E. (2006) Biosorption thermodynamics of Cadmium on coconut copra meal as biosorbent. *Biochemical Engineering Journal*, 30: 117-123.

Horsfall, M.; Abia, A. A and Spiff, A. I. (2006) Kinetic studies on the adsorption of  $\text{Cd}^{2+}$ ,  $\text{Cu}^{2+}$  and  $\text{Zn}^{2+}$  ions from aqueous solutions by cassava (*Manihot sculenta* Cranz) tuber bark waste. *Bioresource Technology*, 97: 283-291.

Hossain, M.A; Ngo, H.H. and Guo, W. (2013) Introductory of Microsoft Excel SOLVER Function - Spreadsheet Method for Isotherm and Kinetics Modelling of Metals Biosorption in Water and Wastewater. *Journal of Water Sustainability*, 3(4)223–237.

Hu, H.; Jiang, B.; Zhang, J. and Chen, X. (2015) Adsorption of perchlorate ion by bio-char produced from *Acidosasa edulis* shoot shell in aqueous solution. *RSC Advances*, 5: 104769–104778.

Huang, X.; Gao, N. and Zhang, Q. (2007) Thermodynamics and kinetics of cadmium adsorption onto oxidized granular activated carbon, *Journal of Environmental Sciences*, 19(11): 1287-1292

Huang, Y.; Li, S.; Chen, J.; Zhang, X. and Chen, Y. (2014) Adsorption of Pb(II) on mesoporous activated carbons fabricated from water hyacinth using  $\text{H}_3\text{PO}_4$  activation: Adsorption capacity, kinetic and isotherm studies. *Applied Surface Science*, 293:160-168.

Hydari, S.; Sharififard, H.; Nabavinia, M. and Parvizi, M.R. (2012) A comparative investigation on removal performances of commercial activated carbon, chitosan biosorbent and chitosan/activated carbon composite for cadmium, *Chemical Engineering Journal*, 193-194: 276-282.

Ibrahim, M. N. M.; Ngah, W. S. W.; Norliyana, M. S.; Daud, W. R. W.; Rafatullah, M.; Sulaiman, O. and Hashim, R. (2010) A novel agricultural waste adsorbent for the removal of lead (II) ions from aqueous solutions. *Journal of Hazardous Materials*, 182: 377-385.

Ipeaiyeda, A.R. and Onianwa, C. P. (2011) Pollution effects of food and beverages effluents on the Alaro River in Ibadan city, Nigeria. *Bulletin of the Chemical Society of Ethiopia*, 25(3): 347-360.

Iqbal, M.; Saeed, A. and Zafar, S. I. (2009a) FTIR Spectrophotometry- kinetics and adsorption isotherms modelling, ion exchange and EDX analysis for understanding the mechanism of Cd<sup>2+</sup> and Pb<sup>2+</sup> removal by mango peel. *Journal of Hazardous Materials*, 164: 161-171.

Iqbal, M.; Schiewar, S. and Cameron, R. (2009b) Mechanistic elucidation and evaluation of biosorption of metal ions by grapefruit peel using FTIR spectroscopy, kinetics and isotherms modeling, cations displacement and EDX analysis. *Journal of Chemical Technology & Biotechnology*, 84 (10): 1516-1526.

Jaouen, G. and Salmain, M. (2015) *Bioorganometallic Chemistry: Applications in drug discovery, biocatalysis and imaging*. Wiley-VCH Verlag-GmbH & Co. KGaA. pp. 373-374.

Kakalanga, S.J.; Jabulani, X.B.; Olutoyin, O.B. and Uteiyin, O.O.(2012) Screening of agricultural waste for Ni(II) adsorption: kinetics, equilibrium and thermodynamic studies. *International Journal of Physical Sciences*, 7(17):2525-2538.

Kannan, N. and Veemaraj, T. (2009) Removal of Lead(II) Ions by Adsorption onto Bamboo Dust and Commercial Activated Carbons -A Comparative Study. *E-Journal of Chemistry*, 6(2), 247-256.

Kannan, N. and Rengasamy, G. (2005) Comparison of cadmium ion adsorption on various activated carbons. *Water, Air and Soil Pollution*, 163(1): 185-201.

Kazemi, F.; Younesi, H.; Ghoreyshi, A.A.; Bahramifar, N. and Heidari, A.(2016) Thiol-incorporated activated carbon derived from fir wood sawdust as an efficient adsorbent for the removal of mercury ion: Batch and fixed bed column studies. *Process Safety and Environmental Protection*, 100: 22-35.

Khah, A.M. and Ansari, R. (2009) Activated charcoal: preparation, characterisation and applications: A review article, *International Journal of ChemTech Research*, 1: 859-864.

Kikuchi, Y.; Qian, Q.; Machida, M. and Tatsumoto, H.(2006) Effect of ZnO loading to activated carbon on Pb(II) adsorption from aqueous solution. *Carbon*, 44(2):195-202.

Kumar, P. S.; Ramakrishnan, K.; Kirupha, D. S. and Sivanesan, S. (2010) Thermodynamic and Kinetic Studies of Cadmium Adsorption from Aqueous Solution onto Rice Husk. *Brazilian Journal of Chemical Engineering*, 27(2): 437-355.

Kumar, P.; Singh, H.; Kapur, M. and Mondal, M.K. (2014) Comparative study of Malathion removal from aqueous solution by agricultural and commercial adsorbents. *Journal of Water Process Engineering*, 3:67-73.

Lagergren, S. (1898) About the theory of so-called adsorption of soluble substances. *Kungliga Svenska Vetenskapsakademiens. Handlingar*, Band 24, No. 4, 1-39.

Langmuir, I. (1918) The adsorption of gases on plane surfaces of glass, mica and platinum. *Journal of American Chemical Society* 40: 1361-1403.

Largitte, L.; Gervelas, S.; Tant, T.; Couespel Dumesnil, P.; Hightower, A.; Yasami, R.; Bercion, Y.; Lodewyckx, P. (2014) Removal of lead from aqueous solutions by adsorption with surface precipitation. *Adsorption*, 20(5-6):689-700.

Largitte, L. and Laminie, J. (2015) Modelling the lead concentration decay in the adsorption of lead onto a granular activated carbon. *Journal of Environmental Chemical Engineering*, 3:474-481.

Li, H.; Dai, Q.; Ren, J.; Jian, L.; Peng, F. and Sun, R. (2016) Effect of structural characteristics of corncob hemicelluloses fractionated by graded ethanol precipitation on furfural production. *Carbohydrate Polymers*, 136:203-209.

Li, X.; Wu, D.; Wang, J.; Zhu, W.; Luo, Y.; Han, C.; Ma, W. and He, S. (2016) Synthesis of large-sized mesoporous silica spheres by pseudomorphic transformation of commercial silica spheres, *Microporous and Mesoporous Materials*, 226 : 309-315.

Li, Y.; Du, Q.; Liu, T.; Sun, J.; Jiao, Y.; Xia, Y.; Xia, L.; Wang, Z.; Zhang, W. Wang, K.; Zhu, H. and Wu, D. (2012) Equilibrium, kinetic and thermodynamic studies on the adsorption of phenol onto graphene. *Materials Research Bulletin*, 47(8):1898-1904.

Liang, S.; Guo, X.; Feng, N. and Tian, Q. (2010) Isotherms, kinetics and thermodynamic studies of adsorption of  $\text{Cu}^{2+}$  from aqueous solutions by  $\text{Mg}^{2+}/\text{K}^{+}$  type orange peel adsorbents. *Journal of Hazardous Materials*, 174: 756 -762.

Lima, L. and Marshall, W. E. (2005) Utilization of turkey manure as granular activated carbon; physical, chemical and adsorptive properties. *Waste Management*, 25: 726-732.

Lin, J. and Wang, L. (2009) Comparison between linear and non-linear forms of first-order and pseudo-second order adsorption kinetic models for the removal of methylene blue by activated carbon. *Frontiers of Environmental Science & Engineering in China*, 3(3): 320-324.

Machida, M.; Aikawa, M. and Tatsumoto, H. (2005) Prediction of simultaneous adsorption of Cu(II) and Pb(II) onto activated carbon by conventional Langmuir type equations. *Journal of Hazardous Materials*, B120: 271-275.

Mailler, R.; Gasperi, J.; Coquet, Y.; Derome, C.; Buleté, A.; Vulliet, E.; Bressy, A.; Varrault, G.; Chebbo, G.; Rocher, V. (2016) Removal of emerging micropollutants from wastewater by activated carbon adsorption: Experimental study of different activated carbons and factors influencing the adsorption of micropollutants in wastewater. *Journal of Environmental Chemical Engineering*, 4(1):1102-1109.

Mittal, A.; Malviya, A.; Kaur, D.; Mittal, J. and Kurup, L. (2007) Studies on the adsorption kinetics and isotherms for the removal and recovery of Methyl Orange from wastewaters using waste materials, *Journal of Hazardous Materials*, 148(1-2) :229-240

Moreno-Castilla, C.; Alvarez-Merino, M.A.; Lopez-Ramon, M.V. and Rivera-Utrilla, J. (2004) Cadmium ion adsorption on different carbon adsorbents from aqueous solutions. Effect of surface chemistry, pore texture, ionic strength, and dissolved natural organic matter. *Langmuir*, 20:8142-8148.

Myers, R.H. (1990) Classical and modern regression with applications, PWSKENT 444-445 (1990) 297-298.

Naumov, S. (2009) Hysteresis Phenomena in Mesoporous Materials, Dissertation of Universitat Leipzig, Available Internet: [http://www.uni-leipzig.de/~gfp/sites/default/files/27-dr\\_sergej\\_naumov/dissertation.pdf](http://www.uni-leipzig.de/~gfp/sites/default/files/27-dr_sergej_naumov/dissertation.pdf) Accessed on 23/1/2016.

Nurchi, V. M. and Villaescusa, I. (2008) Agricultural biomass as sorbents of some trace metals. *Coordination Chemistry Reviews*, 252: 1178-1188.

Nomanbhay, S. M.; and Palanisamy, K. (2005) Removal of Heavy Metal from industrial Wastewater using chitosan coated oil palm shell charcoal. *Electronic Journal of Biotechnology*, 8(1): 43-53.

O'Connell, D. W.; Birkinshaw, C.; O'Dwyer, F. T. (2008) Heavy metal adsorbents prepared from the modification of cellulose: A review. *Bioresource Technology*, 99: 6709-6724.

Olu-Owolabi, B.I.; Diagboya, P.N. and Adebawale, K.O.(2014) Evaluation of pyrene sorption–desorption on tropical soils. *Journal of Environmental Management*, 137:1-9.

Osmari, T.A.; Gallon, R.; Schwaab, M.; Barbosa-Coutinho, E.; Severo Jnr, J.B. and Pinto, J.C. (2013) Statistical analysis of linear and non-linear regression for the estimation of adsorption isotherm parameters. *Adsorption Science and Technology*, 31(5): 433-458.

Paduraru, C.; Tofan, L.; Teodosiu, C.; Bunia, I.; Tudorachi, N. and Toma, O. (2015) Biosorption of Zinc(II) on rapeseed waste: Equilibrium studies and thermogravimetric investigations. *Process Safety and Environmental Protection*, 94: 18-25.

Pagliuca, A. and Mufti, G.J. (1990) Lead poisoning: an age-old problem. *British Medical Journal*, 300:830.

Pamukoglu, Y.; Kargi, F. (2007) Biosorption of Copper (II) ions onto powdered waste sludge in a completely mixed fed-batch reactor: Estimation of design parameters. *Bioresource Technology*, 98: 1155-1162.

Park, D.; Yun, Y. S.; Jo, J. H. Park, J. M. (2006) Biosorption process for treatment of electroplating wastewater containing Cr (IV): Laboratory-scale feasibility Test. *Industrial and Engineering Chemistry Research*, 45: 5059-5065.

Perez-Marin, A.B.; Zapata, V.M.; Ortuno, J.F.; Aguilar, M.; Saez, J and Llorens, M.(2007) Removal of cadmium from aqueous solutions by adsorption onto orange waste. *Journal of Hazardous Materials B*, 122-131.

Pezoti, O.; Cazetta, A.L.; Bedin, K.; Souza, L.S.; Martins, A.C.; Silva, T.L.; Santos-Junior, O.O.; Visentainer, J.V and Almeida, V.C.(2016) NaOH- activated carbon of high surface area produced from guava seeds as a high-efficiency adsorbent for amoxicillin removal: Kinetic, isotherm and thermodynamic studies. *Chemical Engineering Journal*, 288:778-788.

Qiu, H.; Lu, L. V.; Pan, B.; Zhang, Q.; Zhang, W. and Zhang, Q. (2009) Critical Review in Adsorption Kinetic Models. *Journal of Zhejiang University of Science A*, 10(5): 716-724.

Rao, K. S.; Mahapatra, M.; Anand, S. and Venkateswarlu, P. (2010) Review on Cadmium Removal from Aqueous Solutions. *International Journal of Engineering, Science and Technology*, 2(7): 81-103.

Ratkowski, D.A. (1990) Handbook of Nonlinear Regression Models, Marcel Dekker, New York.

Rivera-Utrilla, J.; Sanchez-Polo, M.; Gomez-Serrano, V.; Alvarez, P.M.; Alvim-Ferraz, M.C.M. and Dias, J.M. (2011) Activated carbon modifications to enhance its water treatment applications. An overview. *Journal of Hazardous Materials*, 187:1-23.

Sahoo, S.; Chakraborty, C. K; Behera, P.K. and Mishra, S.C. (2012) FTIR and Raman spectroscopic investigations of Norfloxacin/Carbopol 934 polymeric suspension. *Journal of Young Pharmacist*, 4(3): 138-145.

Sanchez-Polo, M. and Rivera-Utrilla, J. (2002) Adsorbent-Adsorbate Interactions in the Adsorption of Cd(II) and Hg(II) on Ozonized Activated Carbons. *Environmental Science and Technology*, 36:3850-3854.

Sarada, B.; Prasad, M. K.; Kumar, K. K. and Murthy, Ch. V. R. (2014) Cadmium removal by macro algae *Caulerpa fastigiata*: characterisation, kinetic, isotherm and thermodynamic studies. *Journal of Environmental Chemical Engineering*, 2: 1533- 1542.

Sari, A.; Mendil, D.; Tuzen, M. and Soulak, M. (2008) Biosorption of Cd (II) and Cr (III) from aqueous solution by moss (*Hylocomium splendens*) biomass: Equilibrium, kinetic and thermodynamic studies. *Chemical Engineering Journal*, 144: 1-9.

Selomulya, C.; Meeyoo, V. and Amal, R. (1999) Mechanism of Cr (VI) removal from Water by various types of Activated Carbon. *Journal of Chemical Technology & Biotechnology*, 74:111-122.

Sengil, I.A.; Ozacar, M. and Turkmenler,H. (2009) Kinetic and isotherm studies of Cu(II) biosorption on valonia tannin resin. *Journal of Hazardous Materials*, 162:1046-1052.

Shrestha, S.; Son, G.; Lee, S. H. and Lee, T. G. (2013) Isotherm and thermodynamic studies of Zn (II) adsorption on lignite and coconut shell-based activated carbon fibre. *Chemosphere*, 92: 1053-1061.

Simonescu, M.C. (2012) Application of FTIR Spectroscopy in Environmental Studies. In: *Advanced Aspects of Spectroscopy*. Farrukh, A. M. (ed). Intech Publishers, New York, pp 49-84.

Tansel, B. and Nagarajan, P. (2004) SEM study of phenolphthalein adsorption on granular activated carbon. *Advances in Environmental Research*, 8:411-415.

Thirumavalavan, M.; Lai, Y. L. and Lee, J. F. (2011) Fourier transform infrared spectroscopic analysis of fruit peels before and after the adsorption of heavy metal ions from aqueous solution. *Journal of Chemical Engineering Data*, 56:2249-2255.

Tong, S.; Schirnding, Y. E. V. and Prapamontol, T. (2000) Environmental Lead Exposure: A Public Health Problem of Global Dimensions, *Bulletin of the World Health Organisation* 78(9): 1068-1077

Tousandi, H.; Khalidi, A.; Abdennouri, M. and Barka, N. (2016) Activated carbon from *Diplotaxis Harra* biomass: Optimization of preparation conditions and heavy metal removal. *Journal of the Taiwan Institute of Chemical Engineers*, 59:348-358.

Tsai, W. T.; Chang, C. V.; Lin, M. C.; Chien, S. F.; Sun, H. F. and Hsieh, M. F. (2001) Adsorption of acid dye onto activated carbons prepared from agricultural waste bagasse by ZnCl<sub>2</sub> activation. *Chemosphere*, 45: 51-58.

Tsoncheva, T.; Genova, I.; Stoycheva, I.; Spassova, I.; Ivanova, R.; Tsyntsarski, B.; Issa, G.; Kovacheva, D. and Petrov, N. (2015) Activated carbon from waste biomass as catalyst support: formation of active phase in copper and cobalt catalysts for methanol decomposition. *Journal of Porous Materials*, 22(5); 1127-1136.

USEPA (2016) United States Environmental Protection Agency- Cadmium compounds. Available internet: <https://www3.epa.gov/airtoxics/hlthef/cadmium.html> Accessed on 12/04/2016.

Waisberg, M.; Joseph, P.; Hale, B. and Beyersmann, D. (2003) Molecular and cellular mechanisms of cadmium carcinogenesis, *Toxicology*, 192(2–3):95-117.

Wang, J.; Meng, X.; Chen, J.; Yu, Y.; Miao, J.; Yu, W. and Xie, Z. (2016) Desulphurization performance and mechanism study by in situ DRIFTS of activated coke modified by oxidation. *Industrial & Engineering Chemistry Research*, 55: 3790-3796.

Wang, Y.; Tao, Z.; Wu, B.; Xu, J.; Huo, C.; Li, K.; Chen, H.; Yang, Y. and Li, Y. (2015) Effect of metal precursors on the performance of Pt/ZSM-22 catalysts for n-hexadecane hydroisomerization, *Journal of Catalysis*, 322:1-13.

Wasewar, K.L; Kumar, P.; Chand, S.; Padmini, B.N. and Teng, T.T.(2010) Adsorption of cadmium ions from aqueous solution using granular activated carbon and activated clay. *Clean-Soil, Air, Water*, 38(7):649-656.

Weber, W.J and Morris, J.C.(1963) Kinetics of adsorption on carbon from solution. *Journal of the Sanitary Engineering Division*, 89(2); 31-60.

WHO (2010) Exposure to cadmium: a major public health concern. Preventing disease through healthy environments. Available internet: <http://www.who.int/ipcs/features/cadmium.pdf> Accessed on 06/02/2016.

WHO (2011) Cadmium in Drinking water-Background document for development of WHO Guidelines for Drinking-water Quality. Available internet: [http://www.who.int/water\\_sanitation\\_health/dwq/chemicals/cadmium.pdf](http://www.who.int/water_sanitation_health/dwq/chemicals/cadmium.pdf) Accessed on 01/02/2016.

Wong, Y. C.; Szeto, V. S.; Cheung, W. H. and McKay, G. (2004) Adsorption of acid dyes on Chitosan-equilibrium isotherm analysis. *Process Biochemistry* 39: 693-702.

Xi, Y.; Luo, Y.; Luo, J. and Luo, X. (2015) Removal of cadmium(II) from wastewater using novel cadmium ion-imprinted polymers. *Journal of Chemical Engineering Data*, 60: 3253-3261.

Xuan, Z.; Tang, Y.; Li, X.; Liu, Y. and Luo, F. (2006) Study on the equilibrium, kinetics and isotherm of Biosorption of lead ions onto presented chemically modified orange peel. *Biochemical Engineering Journal*, 31: 160-164.

Yaneva, S. L.; Koumanova, B. K. and Georgieva, N. K. (2013). Linear and Nonlinear Regression Methods for Equilibrium modelling of *p*-Nitrophenol Biosorption by *Rhizopus*

*oryzae*: Comparison of Error Analysis Criteria. *Journal of Chemistry*: Article ID 517631, pp 10.  
<http://dx.doi.org/10.1155/2013/517631>

Yang, Y.; Wei, Z.; Xu, C.; Yue, D.; Yin, Q.; Xiao, L. and Yang, L. (2014) Biochar from *Alternanthera philoxeroides* could remove Pb(II) efficiently. *Bioresource Technology*, 171: 227-232.

Zhu, W.; Li, X.; Wu, D.; Yu, J.; Zhou, Y.; Luo, Y.; Wei, K.; Ma, W.(2016) Synthesis of spherical mesoporous silica materials by pseudomorphic transformation of silica fume and its Pb<sup>2+</sup> removal properties, *Microporous and Mesoporous Materials*,222:192-201.

## Figures Captions

**Figure 1:** N<sub>2</sub> adsorption-desorption isotherm (a) and pore size distribution (b) of CGAC

**Figure 2:** SEM micrograph of commercial activated carbon CGAC

**Figure 3:** SEM micrograph of CGAC after Cd(II) sorption (CGAC-Cd)

**Figure 4:** SEM micrograph of CGAC after Pb(II) sorption (CGAC-Pb)

**Figure 5:** EDX spectrum of CGAC adsorbent

**Figure 6:** EDX spectrum of CGAC adsorbent after Cd adsorption (CGAC-Cd)

**Figure 7:** EDX spectrum of CGAC adsorbent after Pb adsorption (CGAC Pb)

**Figure 8:** Thermogravimetric analysis of CGAC adsorbent under N<sub>2</sub>

**Figure 9:** FTIR spectra of CGAC adsorbent

**Figure 10:** FTIR spectra of CGAC adsorbent after Cd(II) adsorption (CGAC-Cd)

**Figure 11:** FTIR spectra of CGAC adsorbent after Pb(II) adsorption (CGAC-Pb)

**Figure 12:** Effect of contact time on metal ion loading on CGAC adsorbent

**Figure 13:** PFO & PSO kinetic models for Cd(II) ion sorption onto CGAC adsorbent

**Figure 14:** PFO & PSO kinetic models for Pb(II) ion sorption onto CGAC adsorbent

**Figure 15:** Kinetic stages in intraparticle diffusion plot of Cd(II) ion sorption on CGAC

**Figure 16:** Kinetic stages in intraparticle diffusion plot of Pb(II) ion sorption on CGAC

**Figure 17:** Langmuir & Freundlich adsorption isotherms for Cd (II) ions on CGAC

**Figure 18:** Langmuir & Freundlich adsorption isotherms for Pb (II) ions on CGAC

## **Tables Captions**

**Table 1:** Characteristics of CGAC adsorbent

**Table 2:** PFO and PSO kinetic parameters for Cd(II) & Pb(II) sorption on CGAC

**Table 3:** Intraparticle diffusion parameters for CGAC sorption of Cd(II) and Pb(II) ions

**Table 4:** Isotherm Parameters for Cd (II) and Pb (II) ions sorption on CGAC

**Table 5:** Comparison of Langmuir constant ( $q_{\max}$ ) with reported literature for Cd(II) ion

**Table 6:** Comparison of Langmuir constant ( $q_{\max}$ ) with reported literature for Pb(II) ion